ARTICLE

Development of machine learning algorithm for loop-mediated isothermal amplification including influence of temperature

Taichi Endoh[1,2], Yuichi Sanekata[1], Kotetsu Kayama[1,3], Daiji Endoh[1,4,5], and Gerry A. Camer*[1,6,7]

[1]Department of Radiation Biology, School of Veterinary Medicine, Rakuno Gakuen University, Ebetsu City, Japan
[2]MATO Corporation Exis Building 4F, 5-26-22 Higashio, Shinagawa-ku, 140-0011, Tokyo, Japan
[3]Kasai Home Care Clinic, TetsuRyuKai Medical Corporation, 101, 8-18-12 Nakakasai, Edogawa-ku, Tokyo,134-0083, Japan
[4]Research Institute for Advanced Nursing Technology, Osaka Metropolitan University 1-1 Gakuen-cho Nakaku, Sakai 599-8231, Japan.
[5]Knowledge Connect (sole proprietor) 4jo-7chome Funino, Minami-ku, Sapporo 061-2284, Japan
[6]Polytechnic University of the Philippines-College of Science, 1016, Sta. Mesa, Manila, Philippines
[7]University of Eastern Philippines-College of Veterinary Medicine, 6400, Catarman, Northern Samar, Philippines

ABSTRACT

To predict amplification in the Loop-Mediated Isothermal Amplification (LAMP) method, a binary model has been developed. This model assesses whether the combination of partial template binding facilitated by multiple primers aligns with a specific signature indicating amplification. For this model, 1512 settings were adjusted, encompassing variations in the extraction oligomer position from the primer, the oligomer length, the number of allowed mismatched bases, and the stringency of the homology position. The optimal set was determined based on the F1 value at a reaction temperature of 60°C, resulting in a value of 0.58. To implement machine learning by amalgamating multiple models, duplicate models were eliminated through cluster analysis. Machine learning using AutoML was performed on 108 distinct models. Consequently, the F1 values were 0.7119 at a reaction temperature of 60°C and 0.7210 at 68°C. The weak correlation between feature importance and the F1 value of the model alone suggests that machine learning

*Corresponding author
Email Address: gercamer@uep.edu.ph
Date received: November 13, 2023
Date revised: April 13, 2024
Date accepted: May 20, 2024
DOI: https://doi.org/10.54645/2024172HJB-85

KEYWORDS

LAMP, machine learning, prediction accuracy, reaction temperature

utilizing this model incorporates numerous models to enhance prediction accuracy.

INTRODUCTION

Loop-mediated isothermal amplification (LAMP), known for its reliability and sensitivity (Notomi et al., 2000; Parida et al., 2008), operates at a constant temperature (~62°C) and yields rapid results, typically within an hour. Widely applied in medicine, agriculture, and the food industry, LAMP is versatile, enabling screening for viral and bacterial mutations, analyzing fungicide resistance, studying microRNA, identifying herbal medicines, detecting plant pathogen vectors, assessing single nucleotide polymorphisms, and identifying genetically modified organisms (Wang et al., 2023; Panno et al., 2020; Li et al., 2017; Srividya et al., 2019). This technique utilizes 18-50 base synthetic primers to specifically amplify DNA sequences (Notomi et al., 2000; Parida et al., 2008), maintaining a constant temperature (60-62°C) for 30 minutes to an hour. Ongoing development of devices for LAMP detection, including point-of-care diagnostics, is underway (Nguyen et al., 2022). Future advancements are expected to focus on incorporating artificial intelligence for its enhanced efficiency (Kayama et al., 2020; Rohaim et al., 2020).

A basic LAMP primer set comprises four synthetic primers derived from six priming regions (Supplementary Figure 1). Consequently, LAMP primer design is more intricate than that of PCR primers. Primer design software, such as GLAPD and LAVA for the LAMP method, relies on alignments to design primers for homologous targets and design primers based on common sequences (Jia et al., 2019; Torres et al., 2011). In these primer design software tools, a perfect primer match is a prerequisite, and homology with other templates is a secondary evaluation criterion used to calculate primer eligibility.

On the other hand, false positives are known to occur in the LAMP method due to amplification at unexpected positions of the template, and methods have been developed to suppress them (Hardinge and Murray, 2019). Amplification by primers lacking complete homology with the template has also been confirmed through programs simulating LAMP primer priming (Salinas and Little, 2012). Based on these reports, to predict whether LAMP amplification will occur, including at unexpected positions (false positive), the information must also consider the formation of incomplete duplexes between the primer and the template.

In the LAMP method, the binding of the four primers to the template at six locations affects the success or failure of amplification; in the LAMP reaction, amplification occurs when DNA synthesis is initiated from each of the six homology regions, but in order, synthesis begins at two locations, the F2 region in the FIP and the B2 region in the BIP, followed by the F3 and B3 (Supplementary Figure 2A). The synthesized strands that were initiated from the F2 region and B2 region become a single strand after the completion of synthesis from F3 and B3 (Supplementary Figure 2B). Then the F1c region in the FIP or B1c region in the BIP becomes double-stranded with the template F1 or B1 region (Supplementary Figure 2B). These are followed by the formation of a dumbbell-shaped partial single strand, and successive amplifications proceed to produce a ladder-shaped amplification product (Supplementary Figure 2C). Since it is difficult to train machine learning with all the complex processes of this time series as the learning information (features), we devised a model that can express the position and strength of the binding of the 6 homology-regions of 4 primers to the template as numerical values (materials and methods). The position, accuracy, and strength of primer binding to the template are expected to vary for each primer/template combination. However, during the model training phase in machine learning, the significance of their contribution to amplification is calibrated, resulting in the development of a model capable of accurate prediction without relying on extraneous features (Mahesh, 2020). The strength of their contribution to amplification is adjusted during the learning process of the learning model so that indicators with a high ratio of contribution to prediction are used more frequently without using unnecessary features. Therefore, when using machine learning to predict amplification, it is possible to proceed with learning by loading a variety of indicators (features), unlike other methods such as kinetics on the resolution curve (Rolando et al., 2020).

The location and direction of primer-template duplex formation have been organized by Torres et al. (2011) as a LAMP signature. We developed mlms-model to estimate features as described in Materials and Methods, Fig. 1). In the in-house experiments, the F1 scores using a single model, ranging from 0.1 to 0.64, were compared with 992 experimental results. The variability in F1 scores (ranging from 0.1 to 0.64) indicates that prediction accuracy varies significantly depending on the model settings. The prediction model with the highest agreement with experimental results achieved an F1 score of 0.64, suggesting that the models can be utilized for machine learning features (Sanekata et al., 2024).

In constructing a machine learning system for predicting LAMP amplification outcomes, it is essential to account for the reaction temperature. While a previous study (Sanekata et al., 2024) proposed a reaction temperature of 68°C, the typical temperature range for the LAMP method is 60°C to 65°C, which significantly influences the results. Therefore, to ensure comprehensive training data, we collected data from amplifications conducted at both 68°C and 60°C. Considering the previously overlooked factor of temperature impact, it is crucial to determine how to incorporate this variable into the prediction algorithm. One approach involves directly integrating temperature effects into the model, while another method entails constructing separate machine learning algorithms for each temperature setting and using their predictions for practical applications. We chose the latter approach to incorporate temperature effects into machine learning. Leveraging AutoML for automated machine learning construction, we developed learning models using the two different sets of training data.

Thus, our approach enabled the integration of primer and template sequence information with temperature settings into a machine learning model, facilitating predictions for LAMP amplification, thereby offering a powerful tool for primer design and distinguishing target genes, even in cases of highly similar bacterial or viral strains.

MATERIALS AND METHODS

Template:
The template for the LAMP method was an artificially synthesized gene, comprising 500 to 560 bases of the V8 region of 16S ribosomal RNA from 31 phyla of bacteria (Supplementary Table 1). The synthesis process followed the published method (Camer et al., 2018; Nishida et al., 2023).

Primer Sets
Primer sets were designed for each synthetic template, with each set comprising F3, FIP, BIP, and B3. The sequence of each primer is provided in Supplementary Table 2. The primer sequences were designed using Primer Explorer 5. The primer sets designed were those predicted by the program to have the

highest amplification potential for each template, but because the 31 templates are highly homologous to each other, the specificity of each primer set to a template cannot be guaranteed. Since this study also examines the mechanism of nonspecific amplification, the resulting low specificity of amplification was judged to be significant for the study.

LAMP Experiment

Amplification experiments were conducted using a Japanese LAMP amplification kit (LAMP MASTER for Turbidity - Visible Dye, Nippon Gene Corporation, Tokyo, Japan). Amplification reactions were carried out at 60°C for 120 minutes, with a template concentration of 10^5 molecules per tube. LAMP products were confirmed by agarose electrophoresis (1.2%, 0.5×TBE) for 30 minutes. Results obtained at 68°C were either validated or referenced from our in-house laboratory experimental analysis (Sanekata et al., 2024).

Classification of LAMP amplification patterns

Amplification was confirmed with certain template and primer combinations in the LAMP experiments. To analyze the mechanism of amplification, amplification patterns were classified based on electrophoresis results (Supplementary Fig.1). Among these, results in which a constant ladder was observed (D, F and T) were considered to be the result of LAMP amplification. Consequently, the analytical evaluation classified D, F and T as positive results and L and a as negative results.

Predictive evaluation index Training data, labels, and learned-models

Basic Concept and Features for Machine Learning

As mentioned in the introduction, the four primers cause LAMP amplification by priming from six regions (Supplement Figure 2 and Figure 3 A-C). In this study, we hypothesized that LAMP amplification occurs when some of the priming regions bind to the template in the correct direction and order (Supplement Figure 3D).

Predictive evaluation index

In order to use LAMP amplification prediction in machine learning, we set as training data that some oligomers of the six priming regions bind to the correct position of the correct template as binary data. The details of the generation of training data are described below. For the training data, set binary values to indicate the compatibility between a primer set and template based on extracted oligomers, alignment stringency, and number of incorrect alignments. The training was performed for the number of settings multiplied by the number of primer set-template combinations, and trained models were created using PyCaret using the training data as the amplification results of each primer set-template.

Setting amplification prediction conditions (APC)

As mentioned above, amplification was predicted basically according to alignment of partial oligomers on priming regions F3,F2,F1,B1,B2,B3. If it is not positive, it is called LAMP negative type. The binary prediction data was used as the training data. Predictions were performed under various conditions as described below. We set a large number of amplification predictions.

- Position from the 3' end of the oligomer sequence to be excised from the priming region (Figure 1 A, Supplement Figure 4, “mg”).
- Length of oligomer sequence excised from the priming region (Figure 1 A, Supplement Figure 4, “ln”).
- Alignment of the excised base sequence to the template (Figure 1 B, Supplement Figure 4, “mut”). To conduct the alignment of the oligomer to the template, SeqKit was employed (Shen et al., 2016).
- Positions of the alignment of extracted oligomer-sequences were in the order, F3, F2, F1, B1, B2, B3, and an additional number of alignment between pair(s) of F3, F2, F1, B1, B2, B3 (Figure 1B, “sr”).

Figure 1A

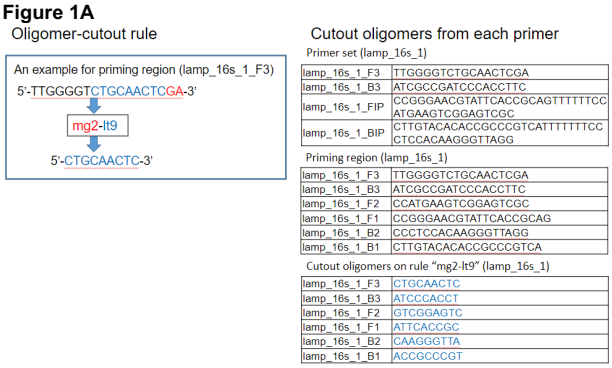

Figure 1B

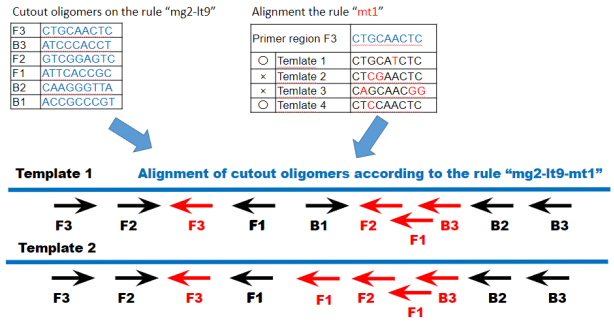

Figure 1: Procedure for predicting primer-template alignment. **(A)** Procedure for cutting out oligomer sequences to be aligned from primer sequences; **(B) Alignment of the excised oligomer sequence onto the template with specified stringency**

Legends:

A: Example of oligomer excision rules (mg: margin, lt: length) and the procedure for excision from the target base sequence (left). Excision of the priming region from the primer sequence and oligomer excision procedure according to the oligomer excision rules (right).

B: Oligomer sequences excised based on the rules (left), and an example of oligomer sequence alignment judgment on the template based on the strictness rule "mt1" (allowing up to one base difference) (right). An example of alignment on a template based on base difference tolerance rules. The black text indicates a normally placed alignment, and the red text indicates an alignment in an unexpected position or direction (bottom).

On these conditions, length of oligomer (ln) was set to 6-18 bases, margin of oligomer from 3’-end of priming region (mg) was set to 0-3 bases, and additional number of alignment between correct alignment (sr) was set to values of 1, 2, 3, 5, 7, and 9. Regarding mt, 0 only (6 bases) to 0-6 (18 bases) was set depending on ln (Supplement Table 3). As a result, a total of 1,512 amplification prediction conditions were set. The amplification prediction conditions were described by a method in which four types of conditions were listed together, such as mg0-ln7-mt1-sr7. For all APCs, 1,512 (sort of APC) x 992 (Number of primer set-template, 31 primer sets x (31 templates and 1 background) = 1,499,904 sets of predictions were performed. The amplification judgments for all APC were compared with the actual amplification (Table 2) to confirm the agreement of the predictions (Figure 2B). From these comparisons, sensitivity and specificity were calculated based on the match with the results of 31 primer sets x 32 templates, so accuracy and F1 values for each APC were also calculated (Table 3 for typical values).

Geobacillus stearothermophilus, inevitably included in the LAMP enzyme extraction process, served as a template sequence alongside the artificially synthesized gene (Supplementary Table 1). This inclusion ensured that the 16S rRNA gene of *Geobacillus stearothermophilus* was present in all templates when predicting the LAMP model match. The prediction was based on the assumption that the 16S rRNA gene of *Geobacillus stearothermophilus,* unavoidably introduced during LAMP enzyme extraction, is present in all templates (column 0 in Table2).

Amplification prediction from primer set, template base sequence, and APC

Amplification determination for each primer set, template, and APC was performed in the following order.

- Oligomer sequences for determination were cut out based on mg and ln from the six priming regions for each primer set (Figure 1A).
- The binding positions of the excised oligomer sequences were aligned on the template according to the mt conditions for each APC (Figure 1B, Figure 2A). In background experiments, the 16S rRNA sequence of Geobacillus stearothermophilus was used as a template sequence.
- Amplification determination based on alignment of the excised oligomer sequences was performed in the following two steps, and if the two conditions were met, the amplification was predicted as positive.
    - For the sense strand of the template, the alignment positions of the extracted oligomers from each priming region are arranged in the order of F3(+), F2(+), F1(-), B1(+), B2(-), B3(-). (Figure 2A).
    - If there are alignments outside the normal order, such as B2(-) and B3(-) (for example F3(+), F2(+),F3(-),F1(-), B1(+), B2(-), F2(-),F1(-),B3(-), B3(-)), the number of alignments that fall between the normal orders is below the number indicated as "sr" (Figure 2A).

Figure 2A

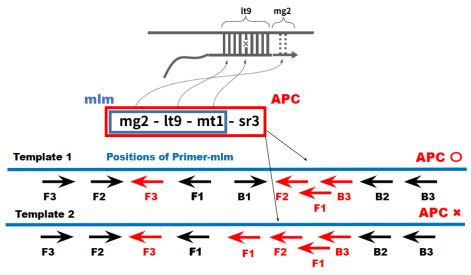

Figure 2B

Template / Primer	1		2		3		4		5	
12	×	○	×	×	×	○	×	○	×	○
13	○	○	×	○	○	×	×	○	×	○
14	○	○	○	○	○	○	○	×	○	○
15	○	○	×	○	×	○	○	○	○	○
16	○	×	×	○	×	○	○	○	○	×

Figure 2: Evaluations of single amplification primer model (APC). **A**. Schematic explanation of mlms-model and APC; **B**. An example of binary classification results of APC and LAMP results

Legends:

A: Configuration and determination of alignment prediction conditions (APC) based on alignment based on mlm (margin, length, mutation) conditions and admissibility rules (sr) for alignment placement.

B: An example of a table showing amplification predictions based on APC converted into truth values and the presence or absence of amplification in experimental results for each combination of primer set and template. Sensitivity and specificity are calculated based on this true/false match.

Character-set for Homology-alignment Analysis

The conditions for LAMP are F3+, F2+, F1c-, B1c+, B2-, and B3-, in that specified order along the sense strand of the template, and the character transformation results in ECBGJL. For instance, if the order of F2+, F3+, B1c-, F3+, B3-, F2+, B1c-, F1c-, B1c+, F3-, B2-, B3-, B1c+ appears in a given string, it is converted to homology characters DEHELCHBGJLG (Supplementary Table 4).

Subsequently, if the string ECBGJL contains six or more consecutive characters from this converted string, the program is executed to extract that segment. Extraction is performed if the sequence of six characters is ECBGJL, even if there are other characters in between (Supplementary Fig. 4B). The acceptable number of intervening homologous positions was set for each condition. For example, homology characters "DEHELCHBGJLG" including HEL between E and C of amplifiable character alignment ECGGJL. Resultantly, "DEHELCHBGJLG" suggested to be amplifiable on the criterion "mg0_lt7_mt1_sr3" but on the criterion "mg0_lt7_mt1_sr2", this homology character suggested not to be amplifiable. The confirmation of whether or not the order of homology positions matched the criteria was conducted using Ruby regular expressions. The program determining the order of homology positions will be published on GitHub.

Clustering conditions

The 1,512 APCs were applied to 992 sets of primer-template combinations, recording 1 if one or more amplification prediction arrangements were present and 0 if none were detected in an APC. This determination is made solely based on the sequence of the primer and template.

In machine learning, experimental results on 992 primers-template combinations serve as labels on training of machine-learning models with APCs.

To make predictions in machine learning, using the 1,512 APC as they are for training is not desirable due to the aim of keeping computational complexity low. Therefore, we clustered the APC, considering them as the same prediction if the amplification prediction patterns for each primers-template match were more than 99% (Supplementary Figure 5A). Matching means that the predictions match for the same Primers-Template pair. As shown in Supplementary Table 6, two APC, namely mg1_ln10_mt0_sr1 and mg3_ln7_mt0_sr5, match more than 99%, and we have shown an example of matching this with some primers and templates (Supplementary Table 5B).

For clustering of 1,512 APC, we selected 1,142,316 combinations for the two sets of 1,512 APC and recorded 1 if the 992 predictions per primers-template matched 99% or more (Supplementary Figure 5A). Then, for each of the 1,142,316 combinations, a data file in abc format was created with the names of the two APC and number '1'. An example of a single line in the abc format is: "mg1_lt7_mt2_sr2 mg0_lt6_mt0_sr1 1" (Supplementary Figure 5B). Clustering from files in abc format was performed by MCL - a cluster algorithm for graphs (Van, 2008, clustering image could be referred to https://micans.org/mcl/). As a result of the MCL program,

clustered APCs were provided in the form of a single line (Supplementary Figure 5B, Supplementary Table 6).

Machine Learning using PyCaret

In this research, a low code PyCaret machine learning technique is used for LAMP amplification prediction. Basically, we accomplished the analysis according to the normal procedure for PyCaret machine learning (Whig et al., 2023). Shortly, after loading a data table, PyCaret automatically splits the data into training and test data, trains 14 classification models (Logisticregression, Ridgeclassifier, Linear discriminant analysis, Random forest classifier, Adaboost classifier, Gradient boosting classifier, Light gradient boosting machine, Extra trees classifier, K neighbors classifier, Decision tree classifier, Naive Bayes, Dummy classifier, Quadratic discriminant analysis and SVM-linear kernel) in parallel, and selects the most appropriate model based on the set evaluation criteria. After selection, we performed an evaluation on the test dataset.

The datatable was constructed with 109 columns and 992 rows, where each row represents a pair of primer-set and template. As the label (target) column, experimental results were set on the left-end of the columns. In the remaining columns, representative APCs of the 108 APC clusters were set as features, and amplification predictions for each primer set-template were entered as binary data in each row. The structure of the data table is schematically shown in Supplementary Table 7.

PyCaret read the table and performed training using the representative 108 APC (Supplementary Table 5 and 6). Training of 14 classification models using modified F1-score (F1) as evaluating index. Precision, Recall, Accuracy, and a F1 were calculated. The Extra trees classifier was used to evaluate the test data as the model that showed the highest modified-F1 value.

Analysis of the amplification process according to model analysis

The binding predictions and experimental results for each search oligomer list based on the confusion matrix were tabulated (Figure 3). Sensitivity, specificity, accuracy, and the F1 were calculated from the tabulated data.

$$Sensitivity = \frac{True\ positive}{(True\ positive\ +\ False\ negative)}$$

$$Specificity = \frac{True\ negative}{(True\ negative + False\ positive)}$$

$$Accuracy\ = \frac{True\ positive\ +\ True\ negative}{(True\ positive\ +\ False\ positive\ +\ False\ negative\ +\ True\ negative)}$$

$$\text{modified } F1 = \frac{2 \times Sensitivity \times Specificity}{(Sensitivity + Specificity)}$$

Figure 3: Confusion matrix

Legends: Calculation procedure for sensitivity, specificity, accuracy and modified F1-score based on confusion matrix.

RESULTS

Determination of the number of clusters

Given that the predictions for the 992 Primer-Template types were in agreement more than 99% of the time, the MCL program predicted 108 clusters. The list of names of APC included in the clusters is shown in Supplementary Table 5. The largest cluster contained 435 APC, while the smallest cluster consisted of 2 APC (Supplementary Table 6). Notably, most APC with oligomers of 8 bases or less taken from the primers were in the largest cluster.

For margin (mg), length of the sequence of interest (lt), and number of tolerated mismatched bases (mt), clusters consisting of more than 60 APC contained multiple APC for all conditions (Supplementary Table 5). This suggests that some conditions made the same prediction even when the margin (mg), length of the sequence of interest (lt), and number of tolerated mismatched bases (mt) were different.

On the other hand, clusters consisting of 6 APC or less were composed of a single mg, lt, or mt. In contrast, for sr, all clusters contained two or more conditions, indicating that the conditions were highly acceptable for sr. The representative APCs selected from each cluster are listed in Table 1.

Table 1: Representative APC

CN	APC	CN	APC	CN	APC	CN	APC
1	mg0_ln10_mt0_sr7	28	mg3_ln17_mt3_sr1	55	mg1_ln8_mt1_sr7	82	mg1_ln14_mt4_sr2
2	mg0_ln10_mt1_sr7	29	mg2_ln18_mt5_sr7	56	mg2_ln10_mt2_sr1	83	mg1_ln15_mt5_sr3
3	mg3_ln18_mt2_sr7	30	mg3_ln16_mt4_sr7	57	mg2_ln12_mt3_sr1	84	mg1_ln17_mt6_sr5
4	mg0_ln17_mt3_sr7	31	mg3_ln17_mt2_sr7	58	mg2_ln13_mt3_sr7	85	mg1_ln18_mt5_sr1
5	mg2_ln12_mt2_sr1	32	mg3_ln18_mt4_sr7	59	mg2_ln13_mt3_sr1	86	mg1_ln8_mt1_sr2
6	mg0_ln12_mt2_sr7	33	mg0_ln13_mt3_sr7	60	mg2_ln14_mt4_sr1	87	mg2_ln10_mt2_sr7
7	mg2_ln12_mt2_sr7	34	mg0_ln16_mt5_sr7	61	mg2_ln15_mt4_sr7	88	mg2_ln12_mt3_sr7
8	mg0_ln14_mt3_sr7	35	mg3_ln8_mt1_sr7	62	mg2_ln15_mt4_sr1	89	mg2_ln13_mt4_sr2
9	mg0_ln16_mt3_sr7	36	mg0_ln12_mt3_sr7	63	mg2_ln17_mt5_sr7	90	mg2_ln14_mt4_sr5
10	mg0_ln17_mt4_sr7	37	mg0_ln18_mt6_sr3	64	mg2_ln17_mt5_sr1	91	mg2_ln15_mt5_sr2
11	mg1_ln17_mt4_sr7	38	mg1_ln12_mt3_sr7	65	mg2_ln18_mt6_sr7	92	mg2_ln16_mt5_sr7
12	mg2_ln16_mt4_sr7	39	mg1_ln18_mt5_sr7	66	mg3_ln11_mt2_sr7	93	mg2_ln16_mt5_sr1
13	mg2_ln18_mt4_sr7	40	mg2_ln8_mt1_sr7	67	mg3_ln12_mt3_sr7	94	mg2_ln16_mt6_sr7

14	mg0_ln11_mt4_sr9	41	mg3_ln15_mt4_sr3	68	mg3_ln13_mt3_sr7	95	mg2_ln17_mt6_sr7
15	mg3_ln15_mt3_sr7	42	mg3_ln18_mt5_sr7	69	mg3_ln13_mt3_sr1	96	mg2_ln17_mt6_sr2
16	mg0_ln11_mt2_sr7	43	mg0_ln14_mt4_sr7	70	mg3_ln14_mt3_sr7	97	mg2_ln18_mt6_sr2
17	mg0_ln15_mt4_sr7	44	mg0_ln8_mt1_sr7	71	mg3_ln14_mt3_sr1	98	mg2_ln8_mt1_sr1
18	mg0_ln16_mt4_sr7	45	mg1_ln11_mt2_sr7	72	mg3_ln17_mt5_sr7	99	mg3_ln10_mt2_sr7
19	mg0_ln17_mt5_sr7	46	mg1_ln11_mt2_sr1	73	mg3_ln6_mt0_sr7	100	mg3_ln12_mt3_sr2
20	mg0_ln18_mt5_sr7	47	mg1_ln13_mt3_sr7	74	mg0_ln10_mt2_sr7	101	mg3_ln14_mt4_sr7
21	mg0_ln6_mt0_sr7	48	mg1_ln13_mt3_sr1	75	mg0_ln13_mt4_sr7	102	mg3_ln14_mt4_sr2
22	mg0_ln9_mt1_sr7	49	mg1_ln16_mt5_sr7	76	mg0_ln13_mt5_sr7	103	mg3_ln15_mt4_sr7
23	mg1_ln14_mt3_sr7	50	mg1_ln16_mt5_sr1	77	mg0_ln14_mt4_sr3	104	mg3_ln16_mt5_sr7
24	mg2_ln14_mt3_sr1	51	mg1_ln17_mt5_sr7	78	mg0_ln18_mt6_sr7	105	mg3_ln16_mt5_sr2
25	mg1_ln15_mt4_sr7	52	mg1_ln17_mt5_sr1	79	mg0_ln8_mt1_sr2	106	mg3_ln17_mt5_sr1
26	mg1_ln16_mt4_sr7	53	mg1_ln18_mt6_sr7	80	mg1_ln10_mt2_sr7	107	mg3_ln18_mt5_sr1
27	mg2_ln11_mt2_sr7	54	mg1_ln18_mt6_sr1	81	mg1_ln14_mt4_sr7	108	mg3_ln18_mt6_sr5

Legend:
992 primer sets - Representative APCs of clusters determined based on 99% or more agreement between amplification predictions using templates.

Results of LAMP amplification experiments at 60°C

The results of LAMP amplification at 60°C are presented in Table 2. The meaning of each symbol is indicated in the Materials and Methods section. Among the amplification patterns, D, F, and T were considered positive amplification results, while all other patterns were deemed negative amplification results (Supplementary Figure 1).

Table 2: Experimental LAMP results at 60°C

Template / Primer	0	1	2	3	4	5	6	7	8	9	10	11	12	13	14	15	16	17	18	19	20	21	22	23	24	25	26	27	28	29	30	31
1	F	F	F	F	F	F	F	F	F	F	F	F	F	F	F	F	F	F	F	F	F	F	F	F	F	F	F	F	F	F	F	F
2	F	F	F	F	F	F	F	F	F	F	F	F	F	F	F	F	F	F	F	F	L	L	F	F	F	L	F	L	F	F	F	F
3	F	F	F	F	F	F	F	F	F	F	F	F	F	F	F	F	F	F	F	F	F	F	F	F	F	F	F	F	F	F	F	F
4	F	F	F	F	F	F	D	F	a	D	D	F	D	F	D	D	F	F	F	F	F	D	F	D	L	D	F	L	D	F	F	L
5	D	D	L	F	F	F	F	L	F	F	F	F	F	F	F	L	F	D	L	L	L	D	F	a	L	F	F	D	F	L	F	a
6	L	L	L	L	L	L	D	L	L	L	L	L	L	L	L	F	L	L	L	a	L	L	L	L	L	L	L	L	L	L	L	a
7	F	F	F	F	F	L	F	F	F	F	F	F	F	F	L	F	F	F	F	F	F	F	F	F	F	F	F	F	F	F	F	F
8	F	T	L	L	L	L	L	F	T	T	F	L	T	L	D	L	F	L	L	D	L	F	F	L	T	F	T	L	F	L	L	a
9	F	F	D	a	L	D	F	D	F	F	a	D	F	F	a	L	a	D	F	D	F	a	F	F	F	F	F	F	F	L	F	F
10	T	T	T	T	T	D	T	T	T	T	T	T	T	T	T	T	T	T	T	T	T	T	T	T	T	T	T	T	T	T	T	T
11	F	F	F	F	F	F	F	F	F	F	F	F	F	F	F	F	F	F	F	F	F	F	F	F	F	F	F	F	F	F	F	F
12	L	L	L	a	L	L	L	L	L	L	a	L	L	L	L	L	L	L	L	L	L	L	L	L	L	L	a	L	L	L	a	L
13	L	F	L	D	a	a	F	L	F	F	F	F	F	L	F	F	D	F	L	L	L	D	L	F	L	F	F	L	L	L	L	L
14	F	F	F	F	F	F	F	F	F	D	F	F	F	D	F	F	F	F	F	F	F	F	F	F	F	F	F	F	F	F	F	F
15	L	D	L	L	L	D	F	F	F	L	F	L	L	L	F	F	F	L	L	L	F	F	D	F	D	F	L	L	L	F	L	L
16	a	F	L	L	L	L	L	L	a	F	L	L	L	a	F	L	F	L	D	L	L	L	L	L	a	F	F	F	L	L	F	F
17	F	F	F	F	F	F	F	F	F	F	F	F	F	F	F	F	F	F	F	F	F	F	F	F	F	F	F	F	F	F	F	F
18	F	F	F	F	F	L	L	F	F	F	F	F	F	F	F	F	F	a	F	a	L	F	F	F	F	D	F	F	F	F	L	L
19	a	L	L	D	L	L	L	F	L	F	L	F	L	L	D	L	a	L	F	L	L	L	L	L	D	L	L	F	F	D	F	F
20	L	F	a	a	L	L	L	L	F	F	L	a	F	L	D	L	L	L	L	L	F	L	L	L	L	F	L	L	F	L	L	F
21	F	F	F	F	F	F	F	F	F	F	L	F	F	a	F	F	F	F	T	F	F	F	F	L	D	F	a	a	F	F	D	F
22	L	D	F	L	L	L	L	L	D	L	L	L	D	F	D	L	L	L	L	D	L	F	L	D	D	D	L	L	L	L	L	L
23	F	F	F	D	D	D	D	D	a	D	D	F	F	D	D	D	a	a	F	D	D	D	F	F	F	F	F	D	a	D	D	F

24	F	F	F	F	F	F	F	F	F	F	F	F	F	F	F	F	F	F	F	F	F	F	F	F	F	F	F	F	F	F	F
25	F	F	F	F	F	F	F	F	F	F	D	F	F	F	F	F	F	D	F	F	F	F	F	F	F	F	F	F	F	F	F
26	D	D	D	D	D	D	D	D	D	D	D	D	D	D	D	D	D	D	D	D	D	D	D	D	D	D	D	D	D	D	D
27	F	F	F	F	F	a	F	a	F	F	a	F	F	F	F	F	F	F	F	F	F	a	F	F	F	F	F	F	F	L	F	F
28	F	F	F	F	a	a	F	F	F	F	F	a	F	F	F	F	F	F	F	F	a	F	F	a	F	a	F	a	D	F	F	F
29	D	L	a	a	a	L	F	D	F	a	F	F	L	F	a	a	a	L	F	F	L	F	L	L	L	L	F	L	L	F	F	D
30	L	L	D	L	L	F	L	L	L	D	D	L	L	L	L	L	a	L	L	L	L	L	L	L	L	D	L	L	L	L	L	L
31	F	F	D	D	D	D	F	D	D	D	D	F	F	D	D	D	F	F	D	F	F	D	D	D	L	F	F	D	F	F	F	F

*Template no “0” means no template in the experiment

Legend:
The meaning of the amplification results for each primer set-template alphabet is listed in Supplementary Figure 1.

Sensitivity, specificity and F1 of APC at 60°C and 68°C

For the 60°C results (Table 2) and the 68°C results (as described in Materials and Methods), sensitivity, specificity, and the F1 were recalculated by reassessing predictions on 992 pairs of Primer-Template. In the previous paper, the absence of a search string (ECBGJL) was excluded from the calculation of sensitivity and other indices. However, in this study, sensitivity, specificity, and the F1 were calculated with the assumption that the absence of a search string (ECBGJL) predicts that LAMP is not applied (see Table 3).

Table 3: Sensitivity, Specificity, Accuracy and modified F1-score at 60°C

mlms	Sensitivity	Specificity	Accuracy	modified F1
mg3_ln16_mt5_sr7	0.60	0.55	0.47	0.58
mg3_ln14_mt4_sr7	0.47	0.65	0.46	0.54
mg2_ln16_mt5_sr7	0.53	0.55	0.44	0.54
mg2_ln17_mt5_sr7	0.48	0.58	0.44	0.52
mg1_ln16_mt5_sr7	0.60	0.46	0.44	0.52
mg3_ln18_mt6_sr5	0.48	0.58	0.44	0.52
mg2_ln13_mt4_sr2	0.52	0.50	0.42	0.51
mg3_ln17_mt5_sr7	0.44	0.59	0.43	0.51
mg2_ln17_mt5_sr1	0.44	0.59	0.43	0.50
mg3_ln16_mt5_sr2	0.44	0.58	0.43	0.50
mg2_ln15_mt4_sr7	0.39	0.68	0.45	0.50
mg2_ln14_mt4_sr5	0.44	0.56	0.42	0.49
mg1_ln16_mt5_sr1	0.48	0.50	0.41	0.49
mg0_ln14_mt4_sr3	0.48	0.50	0.41	0.49
mg2_ln12_mt3_sr7	0.41	0.61	0.43	0.49
mg2_ln18_mt6_sr7	0.58	0.42	0.42	0.49
mg0_ln17_mt5_sr7	0.43	0.57	0.42	0.49
mg1_ln14_mt4_sr7	0.46	0.51	0.41	0.49
mg0_ln14_mt4_sr7	0.49	0.48	0.41	0.49
mg2_ln18_mt6_sr2	0.52	0.44	0.40	0.48
mg2_ln18_mt5_sr7	0.39	0.61	0.42	0.47
mg1_ln14_mt4_sr2	0.43	0.53	0.40	0.47
mg0_ln15_mt4_sr7	0.39	0.60	0.41	0.47

mg2_ln16_mt5_sr1	0.40	0.57	0.41	0.47
mg1_ln18_mt6_sr7	0.59	0.39	0.41	0.47
mg3_ln18_mt5_sr7	0.37	0.63	0.42	0.47
mg2_ln10_mt2_sr7	0.34	0.75	0.46	0.47
mg0_ln16_mt5_sr7	0.46	0.46	0.39	0.46
mg0_ln12_mt3_sr7	0.39	0.57	0.40	0.46
mg2_ln15_mt4_sr1	0.35	0.68	0.43	0.46
mg3_ln17_mt5_sr1	0.37	0.60	0.41	0.46
mg2_ln15_mt5_sr2	0.55	0.39	0.40	0.46
mg2_ln14_mt4_sr1	0.38	0.57	0.40	0.45
mg1_ln18_mt5_sr7	0.36	0.60	0.41	0.45
mg1_ln17_mt5_sr7	0.37	0.58	0.40	0.45
mg1_ln8_mt1_sr7	0.33	0.71	0.44	0.45
mg2_ln17_mt6_sr2	0.61	0.36	0.41	0.45
mg2_ln12_mt3_sr1	0.35	0.63	0.41	0.45
mg1_ln18_mt6_sr1	0.49	0.41	0.38	0.45
mg0_ln10_mt2_sr7	0.35	0.60	0.40	0.45
mg3_ln12_mt3_sr7	0.35	0.61	0.40	0.45
mg2_ln17_mt6_sr7	0.69	0.33	0.42	0.44
mg3_ln14_mt4_sr2	0.33	0.67	0.42	0.44
mg1_ln18_mt5_sr1	0.34	0.61	0.40	0.44
mg1_ln17_mt5_sr1	0.35	0.58	0.39	0.44
mg1_ln17_mt6_sr5	0.58	0.35	0.39	0.44
mg0_ln18_mt5_sr7	0.32	0.67	0.42	0.44
mg0_ln18_mt6_sr7	0.50	0.39	0.38	0.44
mg0_ln18_mt6_sr3	0.48	0.39	0.37	0.43
mg1_ln12_mt3_sr7	0.35	0.53	0.37	0.42
mg3_ln18_mt5_sr1	0.31	0.64	0.40	0.42
mg1_ln10_mt2_sr7	0.29	0.78	0.45	0.42
mg3_ln12_mt3_sr2	0.31	0.64	0.40	0.42
mg3_ln10_mt2_sr7	0.30	0.70	0.42	0.42
mg3_ln15_mt4_sr7	0.30	0.67	0.41	0.41
mg1_ln15_mt4_sr7	0.32	0.57	0.37	0.41
mg2_ln13_mt3_sr7	0.29	0.68	0.41	0.40
mg1_ln15_mt5_sr3	0.52	0.33	0.37	0.40
mg0_ln13_mt3_sr7	0.29	0.65	0.39	0.40
mg0_ln16_mt4_sr7	0.27	0.71	0.42	0.39

mg2_ln10_mt2_sr1	0.26	0.78	0.44	0.39
mg0_ln8_mt1_sr7	0.26	0.78	0.43	0.38
mg3_ln15_mt4_sr3	0.25	0.68	0.39	0.37
mg1_ln13_mt3_sr7	0.26	0.63	0.37	0.36
mg0_ln13_mt4_sr7	0.67	0.24	0.39	0.36
mg2_ln13_mt3_sr1	0.23	0.70	0.39	0.35
mg3_ln16_mt4_sr7	0.23	0.68	0.38	0.35
mg0_ln8_mt1_sr2	0.22	0.79	0.43	0.34
mg1_ln13_mt3_sr1	0.23	0.64	0.36	0.34
mg2_ln16_mt4_sr7	0.22	0.68	0.38	0.34
mg0_ln14_mt3_sr7	0.22	0.72	0.40	0.34
mg1_ln16_mt4_sr7	0.22	0.68	0.38	0.33
mg1_ln14_mt3_sr7	0.22	0.68	0.38	0.33
mg1_ln17_mt4_sr7	0.20	0.69	0.37	0.31
mg2_ln18_mt4_sr7	0.20	0.76	0.40	0.31
mg1_ln8_mt1_sr2	0.19	0.79	0.42	0.31
mg0_ln17_mt4_sr7	0.19	0.77	0.40	0.31
mg2_ln11_mt2_sr7	0.19	0.84	0.44	0.31
mg3_ln13_mt3_sr7	0.18	0.73	0.38	0.29
mg0_ln9_mt1_sr7	0.17	0.86	0.44	0.29
mg0_ln11_mt2_sr7	0.17	0.89	0.45	0.28
mg3_ln18_mt4_sr7	0.17	0.80	0.41	0.28
mg1_ln11_mt2_sr7	0.16	0.90	0.45	0.27
mg3_ln13_mt3_sr1	0.16	0.76	0.38	0.27
mg2_ln14_mt3_sr1	0.15	0.79	0.39	0.25
mg3_ln14_mt3_sr7	0.15	0.81	0.40	0.25
mg1_ln11_mt2_sr1	0.14	0.90	0.45	0.24
mg0_ln16_mt3_sr7	0.14	0.80	0.39	0.24
mg3_ln14_mt3_sr1	0.13	0.84	0.41	0.23
mg0_ln12_mt2_sr7	0.13	0.92	0.45	0.23
mg3_ln15_mt3_sr7	0.13	0.82	0.40	0.22
mg2_ln8_mt1_sr7	0.13	0.89	0.43	0.22
mg3_ln8_mt1_sr7	0.12	0.89	0.43	0.22
mg3_ln11_mt2_sr7	0.12	0.86	0.41	0.22
mg0_ln17_mt3_sr7	0.12	0.86	0.42	0.21
mg2_ln12_mt2_sr7	0.11	0.89	0.43	0.20
g2_ln16_mt6_sr7	0.85	0.10	0.40	0.18

mg2_ln12_mt2_sr1	0.10	0.89	0.42	0.17
mg3_ln17_mt3_sr1	0.09	0.88	0.41	0.16
mg2_ln8_mt1_sr1	0.09	0.95	0.45	0.16
mg0_ln6_mt0_sr7	0.08	0.98	0.46	0.15
mg3_ln6_mt0_sr7	0.08	0.97	0.46	0.14
mg0_ln10_mt1_sr7	0.07	0.96	0.45	0.14
mg3_ln17_mt2_sr7	0.04	0.91	0.40	0.08
mg0_ln13_mt5_sr7	0.98	0.04	0.42	0.07
mg0_ln10_mt0_sr7	0.03	0.99	0.44	0.06
mg3_ln18_mt2_sr7	0.02	0.99	0.43	0.04
mg0_ln11_mt4_sr9	1.00	0.00	0.41	0.00

Legend: Sensitivity, specificity, accuracy and F1 calculated from amplification prediction and amplification results for each APC.

These indices revealed a maximum F1-score of 0.69 at 60°C and 0.64 at 68°C. These results indicate that, for the models used in this study, predictions were more accurate under 60°C conditions (Table 3). Please refer to Sanekata et al., 2024 for the F1 at 68°C.

Machine learning with multiple prediction models

Machine learning with PyCaret was conducted using representative APC from the APC cluster with more than 99% agreement in their predictions (Table 1, Supplementary Figure 5). In PyCaret, the F1 is calculated based on sensitivity and specificity. Machine learning improved the F1 at both 60°C (maximum F1 was 0.69 on a single APC and 0.71 on Extra-tree classifier of PyCaret) and 68°C (maximum F1 was 0.64 on a single APC and 0.72 on Extra-tree classifier of PyCaret) compared to the maximum F1 of an individual APC (Table 4). These results indicate that machine learning enhances the prediction model, with the extent of improvement depending on the reaction temperature of the experiment.

Table 4: Prediction indicators on trained machine learning

Reaction temperature	Sensitivity	Specificity	Accuracy	Modified F1-score
60°C	0.6731	0.7556	0.6980	0.7119
68°C	0.6235	0.8545	0.7886	0.7210

Figure 4 shows the ROC curves generated by PyCaret, which generates a large number of confusion matrices with various thresholds based on negative (class 0) or positive (class 1), and then adds them to the ROC curves using the False positive rate and True positive rate as a scatter plot. The ROC curve has a good balance between positive and negative LAMP at 60°C, but at 68°C, the sensitivity of the class 1 curve increases at low levels of false positives, and the increase in sensitivity slows down in areas with high false positives. This suggests that the 68°C condition is advantageous for detection with few errors, and that 60°C is free of such bias. These ROC curves and AUCs show the predictive ability of the machine learning presented in this study.

Figure 4A

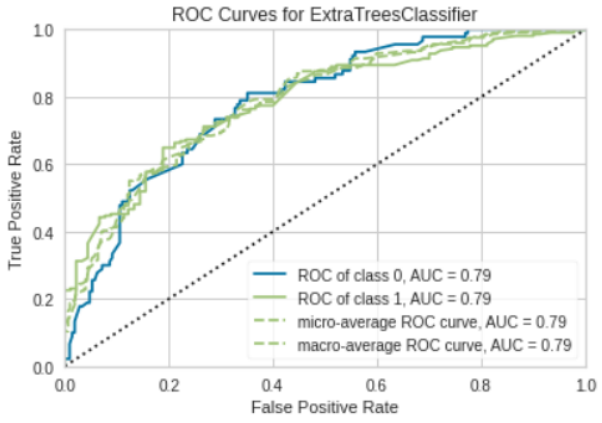

Figure 4B

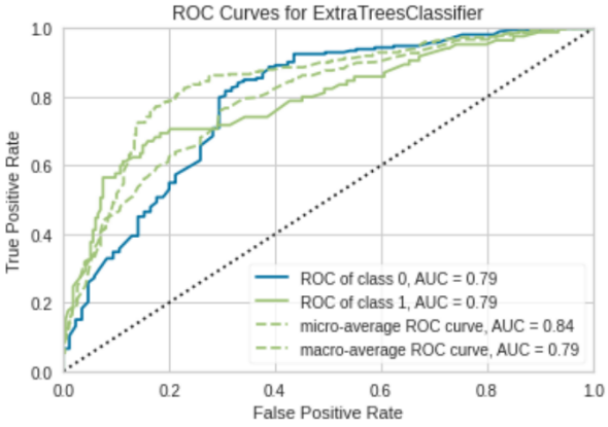

Figure 4: ROC-curves for Extra-tree model

Legends: ROC curve based on APC and experimental amplification results (A: 60°C, B: 68°C).

PyCaret's extra tree model outputs one F1 (Table 4), and at the same time, outputs the degree of contribution to the final prediction as feature importance for all 108 APC in the input data table. On the other hand, for these APCs, the F1 can be calculated by referring to 992 experimental results. If the trained extra tree model utilizes many APCs to produce the final F1, when looking at the correlation between the F1 and feature

importance for APC alone, it may deviate from the simple correlation. It is assumed that there were APCs with high feature importance even though their individual F1s were low. When displaying a scatter plot for each APC with the independent F1 on the horizontal axis and the feature importance in the trained extra tree model on the vertical axis (Figure 5), there are some APCs that have high feature importance even though their individual F1 is low. On the other hand, there were many APCs with low feature importance even though their individual F1 was high. These results show that PyCaret learning skillfully used multiple APCs to make predictions.

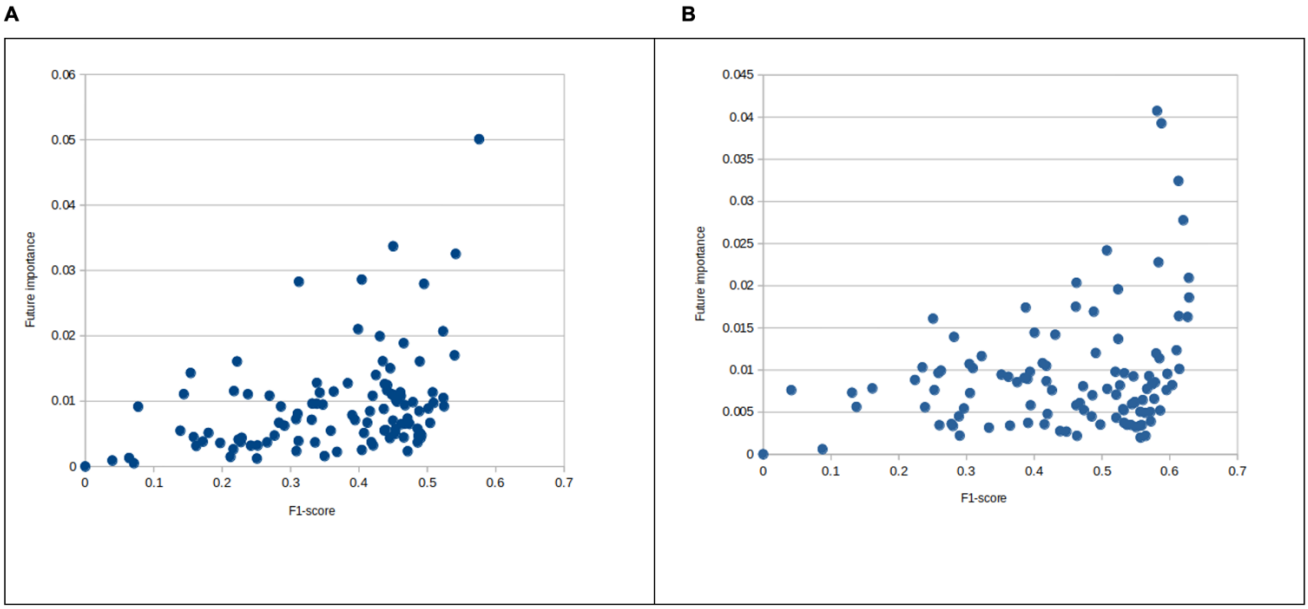

Figure 5: Scatter plot of F1 of individual APCs and feature importance in trained extra tree model

Legend:
For each APC, the F1-score (horizontal axis) is calculated directly based on predictions and experimental results and the feature importance of each APC in the extra tree model trained using PyCaret (A: 60℃, B: 68 ℃).

DISCUSSION

In the context of LAMP prediction, the first consideration for individuals aiming to develop a LAMP method is the primer and template sequences. It is desirable to provide predictions for LAMP amplification, taking into account both sequence information and temperature settings. Specifically, we envision inputting primer candidates and template information from primer design software, such as Primer Explorer V5, GLAPD, and LAVA, into a machine learning model to predict amplification with the target template nucleotide sequence for each candidate (Jia et al., 2019; Torres et al., 2011; Montrasio, 2016).

To achieve this, we established a method of constructing conditions (APC) using margin, length, alignment-accuracy and serial alignment as indicators (mlms-model) to estimate features for training the machine learning model, using a series of amplification results as training data (Supplementary Figure 4). The APC extracts the interrelationship between primers and templates from various angles and creates indicators. This method, involving feature creation through calculations on the original data for machine learning, is akin to methods used for predicting chemical reactions (Coley et al., 2017; Coley et al., 2018). The advantage of using machine learning lies in the accumulation of past data, allowing for fine-tuned improvements and enabling primer design that distinguishes target genes, as desired by the researcher (Mahesh, 2020). This is especially useful when designing primers to distinguish between two similar viral strains with genomic sequences too alike for differential detections (Parida et al., 2005).

We applied the mlms-model proposed in the previous paper (Sanekata et al., 2024) to two temperatures and built machine learning models for two sets of reaction temperatures. To enable this approach, as a first step, we removed duplications of APC by clustering, referring to the predictions on each primer and template sequence used in the experiment (Supplementary Figure 5). Clustering enabled us to create a compact set of features (108 APCs), allowing for efficient machine learning (Table 1). In addition to reducing computation time, removing duplicates is known to increase learning efficiency, as demonstrated in terms of analyzing feature importance in PyCaret, a typical AutoML (Gain and Hotti, 2021). This clustering approach is suggested to be a useful method for increasing the complexity of prediction models in the future, besides improving the accuracy of predictions made by AI models. Since the clustering of APCs in this study was based on the set of primers-templates used in the experiments, it is considered desirable that future LAMP amplification predictions for viral and metagenomic DNA be performed on the data of the templates and the designed primers to be evaluated. Although the increase in primers and templates may lead to an explosive increase in the number of combinations to be compared in APC clustering, the clustering algorithm presented in MCL is extremely efficient and fast, so it may still be useful. It has been suggested that analysis using AutoML improves prediction accuracy by adding and utilizing useful rules for evaluation of prediction (Zender et al., 2023).

Currently, there are 17,800 research papers (Google Scholar 2023/10/25) on viruses and 37,700 (Google Scholar 2023/10/25) on environmental DNA that describe detection methods using the LAMP method. Therefore, if researchers extract primer and template data from these papers along with recorded results, widely applicable machine learning models can be constructed with high precision predictions.

In this study, we present prediction results with F1s of 0.7119 at 60°C and 0.7210 at 68°C. For evaluation of predictions, we used

sensitivity (equal to recall) and specificity to calculate the F1. This indicator was chosen because not only is the detection of the target gene important in the use of the LAMP method, but also the negative result (no amplification) of the LAMP method when the target gene is not present is an important factor in the test (Becherer et al., 2020). In other words, it is suggested that a good balance between sensitivity and specificity is most important when evaluating primers for the LAMP method.

Since the prediction was based on the primer sequence, clustering logically relied on the primer and template sequences only, and the clustering was performed independently of temperature. By adding the temperature effect at the machine learning stage, the machine learning to examine the effect of model temperature took about one hour (Ryzen 5 5600x, 32GB memory with NVIDIA GeForce 1060). It is possible to reduce calculation time by improving the GPU.

In this study, along with related experiments performed in our laboratory, we built a prediction model with the same criteria for six primer binding regions. The present study demonstrated that the number of models can be reduced by clustering, suggesting that machine learning remains feasible even with an increased number of models with clustering. For example, F1c and B1c, F2 and B2, and F3 and B3 are designed with different Tm values in primer design (Jia et al., 2019; Torres et al., 2011; Montrasio, 2016), and it is desirable to construct a prediction model with modified criteria for them. In this study, criteria, i.e., margin of oligomer position, length of oligomer, accepted mutations on homology search, and redundancy of homologous position, were the same for different classes of primers (F1c/B1c, F2/B2, or F3/B3) due to computational limitations. But in the future, it will be possible to organize the increased models by clustering after setting various binding strengths. It is also desirable to introduce into the model factors that may affect the LAMP amplification reaction, such as Gibbs-energy of primer-binding, primer dimers, and hairpin structures in the template (Golyshev et al., 2021; Sugimoto et al., 2000; Lomzov et al., 2015). When such factors are incorporated, the number of models may increase serially, making processing impossible. However, the Primer-Template-based clustering presented in this study is expected to organize the growing number of predictive models and enable analysis, including machine learning.

In predicting amplification by LAMP, the models were constructed by taking into account the contamination of bacterial genomes for LAMP polymerase extraction that existed in the background. Such contamination of DNA and RNA in the background is assumed to be similar to the contamination of host DNA and RNA in virus detection experiments (Kil et al., 2015). The present method that takes background into account can be applied to such conditions and is expected to contribute to the construction of a predictive model for virus detection that assumes the presence of host genomes. By constructing a model that corresponds to the environment of actual detection sites, this research group is considering the possibility of detecting viruses in environments where similar viruses and host RNAs are present (Camer, 2018; Nishida et al., 2023). In particular, the method presented in this study is expected to be effective for avian RNA viruses such as NDV, since a great variety of mutant strains are known, and primer design is required to detect them with high sensitivity while distinguishing between virus strains (Miller et al., 2010).

In recent years, the use of AI in equipment determination criteria has progressed, and the development of low-cost and compact detectors is progressing. In addition to fluorescence detection, which is expensive, the LAMP method allows for a low-cost detection method that detects the scattered light of the LAMP amplification product, and the use of AI makes it possible to make it more compact (Nguyen et al., 2022). Low-cost, highly sensitive, and highly accurate virus detection using such equipment can greatly contribute to controlling pathogens in local communities and epidemic outbreaks (Camer et al., 2018; Molina et al., 1994). The method for predicting LAMP amplification results presented in this study is expected to make a significant contribution to the development of such equipment.

CONCLUSION AND RECOMMENDATION

In predicting LAMP results through primer-template interactions, our analysis with the mcl program revealed 108 clusters of amplifiable alignment of homologous oligomers (APC) featuring shorter oligomers in the largest cluster. Larger clusters consistently provided predictions across diverse conditions, while smaller clusters highlighted varying conditions leading to similar predictions. LAMP experiments at 60°C outpaced those at 68°C, demonstrating improved accuracy for specific patterns. Using representative APC, machine learning featured enhanced F1s at both temperatures. Further refinement of the machine learning approach for LAMP result prediction is suggested, with future studies expanding primer and template sequences and incorporating primer design software inputs for broader model generalizability. Optimizing the clustering process can efficiently handle a larger model count, particularly for diverse primer classes. Once optimally done, this has the potential to revolutionize LAMP primer design for accurate predictions in complex viral detection and environmental DNA analysis.

ACKNOWLEDGMENT

We thank Rakuno Gakuen University for its financial and technical support.

CONFLICT OF INTEREST:

The authors declare no conflict of interest.

CONTRIBUTIONS OF INDIVIDUAL AUTHORS

GAC, KK, and DE conceptualized the study; TE and DE designed the methodology and computer programming; YS conducted lab experiments; and GAC, DE, KK, and TE wrote and enhanced the manuscript.

REFERENCES

Becherer L, Borst N, Bakheit M, Frischmann S, Zengerle R, von Stetten F. Loop-mediated isothermal amplification (LAMP)–review and classification of methods for sequence-specific detection. Analytical Methods. 2020;12(6):717-46.

Camer GA, Oikawa Y, Omaki H, Endoh D. Novel synthetic nucleotides of notifiable dengue (1–4), Japanese encephalitis, yellow fever and Zika flaviviruses. Future Science OA. 2018 Nov 13;5(1):FSO353.

Coley CW, Barzilay R, Jaakkola TS, Green WH, Jensen KF. Prediction of organic reaction outcomes using machine learning. ACS central science. 2017 May 24;3(5):434-43.

Coley CW, Green WH, Jensen KF. Machine learning in computer-aided synthesis planning. Accounts of chemical research. 2018 May 1;51(5):1281-9.

Gain U, Hotti V. Low-code AutoML-augmented data pipeline–a review and experiments. InJournal of Physics: Conference Series 2021 Feb 1 (Vol. 1828, No. 1, p. 012015). IOP Publishing.

Golyshev VM, Pyshnyi DV, Lomzov AA. Calculation of Energy for RNA/RNA and DNA/RNA Duplex Formation by Molecular Dynamics Simulation. Molecular Biology. 2021 Nov;55(6):927-40.

Hardinge P, Murray JA. Reduced false positives and improved reporting of loop-mediated isothermal amplification using quenched fluorescent primers. Scientific reports. 2019 May 14;9(1):7400.

Jia B, Li X, Liu W, Lu C, Lu X, Ma L, Li YY, Wei C. GLAPD: whole genome based LAMP primer design for a set of target genomes. Frontiers in Microbiology. 2019 Dec 13;10:2860.

Kayama K, Hashizume H, Camer GA, Endoh D. An improved gene synthesis method with asymmetric directions of oligonucleotides designed using a simulation program. Techniques. 2020 Jun;69(3):211-9.

Kil EJ, Kim S, Lee YJ, Kang EH, Lee M, Cho SH, Kim MK, Lee KY, Heo NY, Choi HS, Kwon ST. Advanced loop-mediated isothermal amplification method for sensitive and specific detection of Tomato chlorosis virus using a uracil DNA glycosylase to control carry-over contamination. Journal of virological methods. 2015 Mar 1;213:68-74.

Li Y, Fan P, Zhou S, Zhang L. Loop-mediated isothermal amplification (LAMP): A novel rapid detection platform for pathogens. Microbial pathogenesis. 2017 Jun 1;107:54-61.

Lomzov AA, Vorobjev YN, Pyshnyi DV. Evaluation of the Gibbs free energy changes and melting temperatures of DNA/DNA duplexes using hybridization enthalpy calculated by molecular dynamics simulation. The journal of physical chemistry B. 2015 Dec 10;119(49):15221-34.

Mahesh B. Machine learning algorithms-a review. International journal of science and research (IJSR).[https://rb.gy/9of5xh]. 2020 Jan;9(1):381-6.

Miller PJ, Decanini EL, Afonso CL. Newcastle disease: evolution of genotypes and the related diagnostic challenges. Infection, genetics and evolution. 2010 Jan 1;10(1):26-35.

Molina HA, Peña E, Camer GA, and Padilla MA. An outbreak of hemorrhagic septicemia among carabaos in Northern Samar. Philippine journal of veterinary medicine. 1994 Jan 31(1): 27-31.

Montrasio C. Development of a Software Application for Loop-Mediated Isothermal Amplification (LAMP) Primer Design.

Nguyen HQ, Bui HK, Phan VM, Seo TS. An internet of things-based point-of-care device for direct reverse-transcription-loop mediated isothermal amplification to identify SARS-CoV-2. Biosensors and bioelectronics. 2022 Jan 1;195:113655.

Nishida Y, Kayama K, Endoh T, Hanazono K, Camer GA, Endoh D. PCR-based gene synthesis with overlapping unisense-oligomers asymmetric extension supported by a simulator for oligonucleotide extension achieved 1 kbp dsDNA. BioTechniques. 2023 Jun(0).

Notomi T, Okayama H, Masubuchi H, Yonekawa T, Watanabe K, Amino N, Hase T. Loop-mediated isothermal amplification of DNA. Nucleic acids research. 2000 Jun 15;28(12):e63-.

Panno S, Matić S, Tiberini A, Caruso AG, Bella P, Torta L, Stassi R, Davino S. Loop mediated isothermal amplification: principles and applications in plant virology. Plants. 2020 Apr 6;9(4):461.

Parida M, Horioke K, Ishida H, Dash PK, Saxena P, Jana AM, Islam MA, Inoue S, Hosaka N, Morita K. Rapid detection and differentiation of dengue virus serotypes by a real-time reverse transcription-loop-mediated isothermal amplification assay. Journal of clinical microbiology. 2005 Jun;43(6):2895-903.

Parida M, Sannarangaiah S, Dash PK, Rao PV, Morita K. Loop mediated isothermal amplification (LAMP): a new generation of innovative gene amplification technique; perspectives in clinical diagnosis of infectious diseases. Reviews in medical virology. 2008 Nov;18(6):407-21.

Rohaim MA, Clayton E, Sahin I, Vilela J, Khalifa ME, Al-Natour MQ, Bayoumi M, Poirier AC, Branavan M, Tharmakulasingam M, Chaudhry NS. Artificial intelligence-assisted loop mediated isothermal amplification (AI-LAMP) for rapid detection of SARS-CoV-2. Viruses. 2020 Sep 1;12(9):972.

Rolando JC, Jue E, Barlow JT, Ismagilov RF. Real-time kinetics and high-resolution melt curves in single-molecule digital LAMP to differentiate and study specific and non-specific amplification. Nucleic acids research. 2020 Apr 17;48(7):e42-.

Salinas NR, Little DP. Electric LAMP: virtual loop-mediated isothermal amplification. International scholarly research notices. 2012;2012.

Sanekata Y, Kayama K, Endoh T, Endoh D, and Camer GA. Development of a LAMP Simulation and Selection Pipeline to Predict Primer Success. Philippine journal of veterinary medicine. 2024 Jan 8; 61 (1): 26-38 Online: https://rb.gy/ba8ob3 and https://pjvm-ph.org/2024/01/08/volume-61-issue-1/

Shen W, Le S, Li Y, Hu F. SeqKit: a cross-platform and ultrafast toolkit for FASTA/Q file manipulation. PloS one. 2016 Oct 5;11(10):e0163962.

Srividya A, Maiti B, Chakraborty A, Chakraborty G. Loop mediated isothermal amplification: a promising tool for screening genetic mutations. Molecular diagnosis & therapy. 2019 Dec;23(6):723-33.

Sugimoto N, Nakano M, Nakano SI. Thermodynamics−structure relationship of single mismatches in RNA/DNA duplexes. Biochemistry. 2000 Sep 19;39(37):11270-81.

Torres C, Vitalis EA, Baker BR, Gardner SN, Torres MW, Dzenitis JM. LAVA: an open-source approach to designing LAMP (loop-mediated isothermal amplification) DNA signatures. BMC bioinformatics. 2011 Dec;12:1-7.

Van Dongen S. Graph clustering via a discrete uncoupling *process. SIAM Journal on matrix analysis and applications. 2008;30(1):121-41.*

Wang J, Cheng S, Yi L, Cheng Y, Yang S, Xu H, Li Z, Shi X, Wu H, Yan X. Detection of mink enteritis virus by loop-mediated isothermal amplification (LAMP). Journal of virological methods. 2013 Feb 1;187(2):401-5.

Whig, P, Gupta, K, Jiwani, N, Jupalle, H, Kouser, S, Alam, N. A novel method for diabetes classification and prediction with Pycaret. Microsystem technologies. 2023; 29(10), 1479-87.

SUPPLEMENTARY INFORMATION

Supplementary Table 1: Nucleotide sequences of synthesized templates used for LAMP experiments

Template Number	Phylum	Nucleotide Sequence
1	Actinobacteria	CCTTACCTGGGCTTGACATATACAGGATCGCTGCAGAGATGTAGTTTCCCTTGTGGTCTGTATACAGGTGGTGCATGGTTGTCGTCAGCTCGTGTCGTGAGATGTTGG GTTAAGTCCCGCAACGAGCGCAACCCTTGTCTTATGTTGCCAGCACACTWTGGTGGGGACTCATGAGAGACTGCCGGGGTTAACTCGGAGGAAGGTGGGGATGAC GTCAAATCATCATGCCCCTTATGTCCAGGGCTTCACACATGCTACAATGGTCGGTACAACGCGCTGCGAGCCTGTGAGGGTGAGCGAATCGCTGAAAGCCGGCCTCA GTTCGGATTGGGGTCTGCAACTCGACCCCATGAAGTCGGAGTCGCTAGTAATCGCAGATCAGCAACGCTGCGGTGAATACGTTCCCGGGCCTTGTACACACCGCCCG TCAAGTCACGAAAGTTGGTAACACCCGAAGCCAGTGGCCTAACCCTTGTGGAGGGAGCTGTCGAAGGTGGGATCGGCGATTGGGACTAAGTCGTAACAAGGTAGCC GTACCGGAAGGTGCGGCTGGATCACCTCCTTT
2	Spirochaetes	CGATGATACGCGAAAAACCTCACCTAGGCTTGACATGGAGTGGAATCATGTAGAGATACATGAGCCTTCGGGCCGCTTCACAGGTGCTGCATGGTTGTCGTCAGCTC GTGTCGTGAGATGTTGGGTTAAGTCCCGCAACGAGCGCAACCCTCACCTTATGTTGCCATCATTCAGTTGGGCACTCGTAAGGAACTGCCGGTGACAAACCGGAGGA AGGCGGGGATGACGTCAAATCCTCATGGCCTTTATGTCTAGGGCAACACACGTGCTACAATGGCCGGTACAAAGGGTAGCCAACTCGCGAGGGGGAGCTAATCTCA AAAATCCGGTCCCAGTTCGGATTGGAGTCTGCAACTCGACTCCATGAAGTCGGAATCGCTAGTAATCGCGGATCAGCATGCCGCGGTGAATACGTTCCCGGACCTTGT ACACACCGCCCGTCACACCACCTGAGTGGGGAGCACCCGAAGTGGTCTTTGCCAACCGCAAGGAAGCAGACTACTAAGGTGAAACTCGTGAAGGGGGTGAAGTCGT AACAAGGTAGCCGTATCGGAAGGTGC
3	Synergistetes	GTTTGACATGCAGGTGGTACGAGCCTGAAAGGGCGAGGACCGCATCTTCGGATGCGGAGCCTGCACAGGTGCTGCATGGCTGTCGTCAGCTCGTGTCGTGAGATGT TGGGTTAAGTCCCGCAACGAGCGCAACCCCTGCGCCTAGTTGCCATCAGTTAGGCTGGGCACTCTAGGCGGACTGCCGGCGACAAGTCGGAGGAAGGTGGGGATGA CGTCAAGTCATCATGGCCTTTAAGCCCAGGGCGACACACGTGCTACAATGGCCAGCACAGAGGGCTGCAAGTCCGCGAGGACAAGCGAATCCCTTAAAGCTGGTCTC AGTTCGGATTGCAGTCTGCAACTCGACTGCATGAAGCCGGAATCGCTAGTAATCGCCGGTCAGCCATACGGCGGTGAATACGTTCCCGGGCCTTGTACACACCGCCC GTCACACCACCCGAGTTGGGTGCTCCCGAAGCCGCCGGCCCAACCCCGTAAGGGGAGGGAGGCGTCGAAGGAGTGTCTGATAAGGGGGGTGAAGTCGTAACAAGG TAGCCGTACCGGAAGGTGCGGCTGGATCACCT
4	Dictyoglomi	TAAGCGAAGAACCTTACCAGGGCTTGACATGCAGGCTGTAAGCTCACTCGAAAGGGTGAGTGCCAAATAGGGGGTTTCCCCTATTTGGAGCCTGCACAGGTGGTGC ATGGCTGTCGTCAGCTCGTGTCGTGAGATGTTGGGTTAAGTCCCGCAACGAGCGCAACCCCTGCCCTTAGTTGCCAGCGGGTAAAGCCGGGCACTCTAAGGGGACTG CCGGCGAAGAGCCGGAGGAAGGTGGGGATGACGTCAAGTCAGTATGCCCCTTATGCCCTGGGCTACACACGCGCTACAATGGGTGGTACAGAGGGGAGCGAAGCC GCGAGGCGGAGCGAATCCCTAAAGCCACCCCCAGTTCAGATCGCAGGCTGCAACTCGCCTGCGTGAAGGCGGAATCGCTAGTAACCGCAGATCAGCCACGCTGCGG TGAATACGTTCTCGGGCCTTGTACACACCGCCCGTCACACCACGAGAGTCCGCAACACCCGAAGTCAGGCGAAGAGCCTGCCGAAGGTGGGGCGGATGATTGGGGT GAAGTCGTAACAAGGTAGCCGTACCGGAAGGTGCGGC
5	Thermodesulfobacteria	GAGCACGTGGTTTAATTCGATGCAAAGCGAAGAACCTTACCTGGGTTTGACATGCTAGGGGACCCCTCAGAGATGAGGGGGTGCCCGGGCTTTGCCTGGGAGCCCT AGCACAGGTGCTGCATGGCTGTCGTCAGCTCGTGTCGTGAGATGTTGGGTTAAGTCCCGCAACGAGCGCAACCCTTGCCCTTAGTTGCCAGCGGGTAGAGCCGGGCA CTCTAGGGGGACTGCCGGGGACAACCCGGAGGAAGGGGGGGATGACGTCAAGTCATCATGGCCCTTATGCCCAGGGCTACACACGTGCTACAATGGGCGGTACAG AGGGAAGCGAACCCGTAAGGGGGAGCAAATCCCAGAAAGCCGCTCTCAGTACGGATCGGGGTCTGCAACTCGACCCCGTGAAGCCGGAATCGCTAGTAACGGCGG ATCAGCATGCCGCCGTGAATACGTTCCCGGGCCTTGTACACACCGCCCGTCACACCACGGGAGCTGGCTCTGCCCGAAGTCGCTATCCCAACCCCCGGAAGGGGGAG GGAGGCGCCGACGGCAGGGCTGGTGACTGGGGTGAAGTCGTAAC
6	Elusimicrobia	TTAAAACTCAAAGGAATTGACGGGGACCCGCACAAGAGGTGGATTATGTGGTTTAATTTATGAAAGTAGATGTGATTCGCAAGAAAGCCAGCCGAGGTGCTGCATG GTTGTCGTCAGCTCGTGTCGTGAGATGTTGGGTTAAGTCCCGCAACGAGCGCAACCCCTATTCTGTGTTGCCTAGCAATAGGATCTCTCAGAAGACTGCCGCGGATAA CGTGGAGGAGTAATACAATGGCATAGACAGAGGGCAGCAATATCGCGAGATGGAGCCAATCCCTAAACTATGCCCCAGTTCAGATTGCAGGCTGCAATTCGCCTGC ATGAAGCCGGAATCTCTAGTAATCGCAGATCAGCACGCTGCGGTGAATACGTTCCCGGGTCTTGTACACACCGCCCGTCACACCACGAAAGTTAATTGCAACAGAAG TGCTCAGGTCGTCTGGGCCCTAAGTTG
7	Chlorobi	CAACGCGAAGAACCTTACCTGGGCTTGATATTGCAGCTAAACTCATTGAAAGATGAGGTCCTTCGGGAAGCTGTAACAGGTGCTGCATGGCTGTCGTCAGCTCGTGT CGTGAGATGTTGGGTTAAGTCCCGCAACGAGCGCAACCCCTACAATTAGTTACTAACAGGTTAAGCTGAGGACTCTAATTGAACTGCCTACGCAAGTAGTGAGGAAG GAGGGGATGACGTCAAGTCCTCATGGCCCTTACGCCCAGGGCCACACACGTGATACAATGGTAGCTACAGAGGGCAAAGCCGCGAGGCAGAGGAAATCCCAAAAA AGCTATCTCAGTCCGGATCGGAGTCTGCAACTCGACTCCGTGAAGTTGGAATCGCTAGTAATCGCAGATCAGCACGCTGCGGTGAATGTGTTCCCGGGCCTTGTACAC ACCGCCCGTCAAGTCATGGAAGTCAGGAGTACCCAAAGACGCTCGCGCGTTTAAGGTAAGACTGGTAACTGGGACTAAGTCGTAACAAGGTAGCCGTACCGGAAGG TGCGGCTGGATCACCTCCTTT
8	Verrucomicrobia	AGAACCTTACCTGGGCTTGACATGTAATGAACAACATGTGAAAGCATGCGACTCTTCGGAGGCGTTACACAGGTGCTGCATGGCCGTCGTCAGCTCGTGTCGTGAGA TGTTTGGTTAAGTCCAGCAACGAGCGCAACCCCTGTTGCCAGTTACCAGCACGTGAAGGTGGGGACTCTGGCGAGACTGCCCAGATCAACTGGGAGGAAGGTGGGG ACGACGTCAGGTCAGTATGGCCCTTATGCCCAGGGCTGCACACGTACTACAATGCCCAGTACAGAGGGGGCCGAAGCCGCGAGGCGGAGGAAATCCTAAAAACTGG GCCCAGTTCGGACTGTAGGCTGCAACCCGCCTACACGAAGCCGGAATCGCTAGTAATGGCGCATCAGCTACGGCGCCGTGAATACGTTCCCGGGTCTTGTACACACC GCCCGTCACATCATGGAAGCCGGTCGCACCCGAAGTATCTGAAGCCAACCGCAAGGAGGCAGGGTCCTAAGGTGAGACTGGTAACTGGGATGAAGTCGTAACAAG GTAGCCGTAGGGGAACCTGCGGCTGGATCACCTCCTTT
9	Deinococcus-Thermus	CGCGAAGAACCTTACCAGGCCTTGACATGCTAGGGAACCCGGGTGAAAGCCTGGGGTGCCCGCGAGGGAGCCCTAGCACAGGTGCTGCATGGCCGTCGTCAGCTCG TGCCGTGAGGTGTTGGGTTAAGTCCCGCAACGAGCGCAACCCCCGCCGTTAGTTGCCAGCGGTTCGGCCGGGCACTCTAACGGGACTGCCCGCGAAAGCGGGAGGA AGGAGGGGACGACGTCTGGTCAGCATGGCCCTTACGGCCTGGGCGACACACGTGCTACAATGCCCTACAAAGCGATGCCACCCGGCAACGGGGAGCTAATCGCAAA AAGGTGGGCCCAGTTCGGATTGGGGTCTGCAACCCGACCCCATGAAGCCGGAATCGCTAGTAATCGCGGATCAGCCATGCCGCGGTGAATACGTTCCCGGGCCTTGT ACACACCGCCCGTCACGCCATGGGAGCGGGCTCTACCCGAAGTCGCCGGGAGCCTACGGGCAGGCGCCGAGGGTAGGGCCCGTGACTGGGGCGAAGTCGTAACAA GGTAGCTGTACCGGAAGGTGCGGCTGGATCACCTCCTTT

10	Ignavibacteriae	CGCGAAGAACCTTACCTAGGCTTGAAAAGCAGGCGACCGGGTGTGAAAGCACCCTTCCCTTCGGGGCGCCTGTACAGGTGCTGCATGGCTGTCGTCAGCTCGTGCCG TGAGGTGTTGGGTTAAGTCCCGCAACGAGCGCAACCCCTACCATTAGTTGCCATCAGGTTAAGCTGGGCACTCTAATGGGACTGCCTACGCAAGTAGTGAGGAAGGT GGGGATGACGTCAAGTCAGCATGGCCCTTACGCCTAGGGCTACACACGTGCTACAATGGGTGCTACAACGGGTAGCGAAACCGCGAGGTGGAGCCAATCCCTAAAA AGCATCCTCAGTTCGGATTGGAGTCTGCAACCCGACTCCATGAAGCTGGAATTGCTAGTAATCGCGCATCAGCACGGCGCGGTGAATACGTTCCCGGGCCTTGTACAC ACCGCCCGTCAAGCCATGGAAGCCGGGGGTACCCGAAGTCAGTGACCCAACTCCGCCTCGGCGGAGAGGGAGCTGCCGAAGGTAAAACCGGTGACTGGGGCTAAG TCGTAACAAGGTAGCCGTACCGGAAGGTGCGGCT
11	Gemmatimonadetes	CTTACCCAGGCTTGACATGTACGAGAAAGCCTCTGGAAACAGGGGCCCCTCTTCGGAGCTCGTGCACAGGTGCTGCATGGCTGTCGTCAGCTCGTGTCGTGAGATGT TGGGTTAAGTCCCGCAACGAGCGCAACCCTTGCCCTTAGTTACCAGCGAGTAAAGTCGGGGACTCTAGGGGGACTGCCGGTGCCAAACCGGAGGAAGGTGGGGAC GACGTCAAGTCATCATGGTCCTTACGTCTGGGGCTACACACGTGCTACAATGGCCGGTACAGAGGGCTGCGAAAGAGCAATCTGGAGCCAATCCCTAAAGCCGGCCT CAGTTCGGATTGTCGTCTGCAACTCGACGGCATGAAGCTGGAATCGCTAGTAATCGCGGATCAGCGACGCCGCGGTGAATACGTTCCCGGGCCTTGTACACACCGCC CGTCACGCCATGGAAGCTGTGAGCGCCCGAAGTCGGTGCAGGAACCCGCAAGGGGCCAAGCCGCCTAAGGCGAGCGCAGTGACTGGGGCGAAGTCGTAACAAGGT AGCCGTAGGGGAACCTGCGGCTGGATCACCTCCTTT
12	Proteobacteria	AGAACCTTACCTACTCTTGACATCCAGAGAACTTAGCAGAGATGCTTTGGTGCCTTCGGGAACTCTGAGACAGGTGCTGCATGGCTGTCGTCAGCTCGTGTTGTGAAA TGTTGGGTTAAGTCCCGCAACGAGCGCAACCCTTATCCTTTGTTGCCAGCGGTTAGGCCGGGAACTCAAAGGAGACTGCCAGTGATAAACTGGAGGAAGGTGGGGA TGACGTCAAGTCATCATGGCCCTTACGAGTAGGGCTACACACGTGCTACAATGGCATATACAAAGAGAAGCGACCTCGCGAGAGCAAGCGGACCTCATAAAGTATGT CGTAGTCCGGATTGGAGTCTGCAACTCGACTCCATGAAGTCGGAATCGCTAGTAATCGTGGATCAGAATGCCACGGTGAATACGTTCCCGGGCCTTGTACACACCGC CCGTCACACTTACCACTTTGTGATTCATGACTGGGGTGAAGTCGTAACAAGGTAACCGTAGGGGAACCTGCGGTTGGAT
13	Firmicutes	GAAGCAACGCGAAGAACCTTACCAGGTCTTGACATCCTCTGAAAACCCTAGAGATAGGGCTTCTCCTTCGGGAGCAGAGTGACAGGTGGTGCATGGTTGTCGTCAGC TCGTGTCGTGAGATGTTGGGTTAAGTCCCGCAACGAGCGCAACCCTTGATCTTAGTTGCCATCATTAAGTTGGGCACTCTAAGGTGACTGCCGGTGACAAACCGGAG GAAGGTGGGGATGACGTCAAATCATCATGCCCCTTATGACCTGGGCTACACACGTGCTACAATGGACGGTACAAAGAGCTGCAAGACCGCGAGGTGGAGCTAATCT CATAAAACCGTTCTCAGTTCGGATTGTAGGCTGCAACTCGCCTACATGAAGCTGGAATCGCTAGTAATCGCGGATCAGCATGCCGCGGTGAATACGTTCCCGGGCCTT GTACACACCGCCCGTCACACCACGAGAGTTTGTAACACCCGAAGTCGGTGGGGTAACCTTTTTGGAGCCAGCCGCCTAAGGTGGGACAGATGATTGGGGTGAAGTC GTAACAAGGTAGCCGTATCGGAAGGT
14	Fibrobacteres	AATTCGAAGCAACGCGCAGAACCTTACCAGGGTTTGACATGGGAACGCCGCGGCGAGAGATCGCCGTTTTGCAGCAATGCAACGTTCCGCACAGGTGCTGCATGGC TGTCGTCAGCTCGTGTCGTGAGATGTTGGGTTAAGTCCCGCAACGAGCGCAACCCACGTTTCCAGTTGCCACCCGCAAGGGGGCCCTCTGGAGAGACTGCCGGGGAC AACCCGGAGGAAGGTGTGGATGACGTCAAGTCCTCATGGCCCTTACATCCTGGGCTACACACGTGCTACAATGGTCGGTACAATGGGTCGCAACGCCGCGAGGCGG AGCCAATCCTCAAAGCCGTCCTCAGTTCGGATCGGAGTCTGCAACTCGACTCCGTGAAGCTGGAATCGCTAGTAATCGTGGGTCAGCACACCACGGTGAATACGTTCC CGGGCCTTGTACACACCGCCCGTCAAGCCATGGGAGAAGGGAGTGCTCTAAGTCGTGCAAGCGCCTAAAGCAAGACCTTTGACTGGGGCTAAGTCGTAACAAGGTA GCCGTACCGGAAGGTGCGGCTGGATTACCT
15	Acidobacteria	AATGGGTCTGTATATAGGTGCTGCATGGCTGTCGTCAGCTCGTGTCGTGAGATGTTGGGTTAAGTCCCGCAACGAGCGCAACCCTTATCTCCAGTTGCTACCATTTAG TTGAGCACTCTGGCGAAACCGCCTCGGATAACGGGGAGGAAGGTGGGGATGACGTCAAGTCCTCATGGCCTTTATGTCCAGGGCTACACACGTGCTACAATGGCCG GTACAAACCGCTGCAACCCCGCGAGGGTGAGCTAATCGGAAAAAGCCGGCCTCAGTTCGGATTGGAGTCTGCAACTCGACTCCATGAAGCTGGAATCGCTAGTAATC GTGGATCAGCATGCCACGGTGAATACGTTCCCGGGCCTTGTACACACCGCCCGTCACATCACGAAAGGTGTAATTCATGATTGGGGTGAAGTCGTAACAAGGTAGCC GTAGGAGAACCTGCGGCTGGATCACCT
16	Calditrichaeota	TGGTTTAATTCGATGCAACGCGAAGAACCTTACCGGGGTTTGACATGCCGATGACGTCACGGGAGACCGTGATTCCCTTCGGGGCGTCGGCACAGGTGCTGCATGGC TGTCGTCAGCTCGTGTCGTGAGATGTTGGGTTAAGTCCCGCAACGAGCGCAACCCCTGCCTCTAGTTACCATCGGTTCAAGCCGGGGACTCTAGAGGGACTGCCGGC GATAAGCTGGAGGAAGGTGGGGATGACGTCAAGTCCTCATGGCCCTTACACCCCGGGCTACACACGTGCTACAATGGCCGGTACAGCGAGTTGCGAAACCGCGAGG TGGAGCCAATCTCTAAAAACCGGTCTCAGTTCGGATTGCAGTCTGCAACTCGACTGCATGAAGTCGGAATCGCTAGTAATCGCGGATCAGCATGCCGCGGTGAATAC GTTCCCGGGCCTTGTACACACCGCCCGTCACGCCATGGAAGTCGGCAGTACCCGAAGCCCCCGCATTAGCGGGGTCGAAGGTAAGGCCGATGACTGGGGCGAAGTC GTAACAAGGTAGCCGTACCGGAAGGTGCGG
17	candidateNC10	GTGGTTTAATTCGAAGCAACGCGAAGAACCTTACCAGGGCTTGACATCCCGCTGACCGCCCCAGAGATGGGGCTTCCCTCCTTTCGGAGGGCAGCGGTGACAGGTGG TGCATGGTTGTCGTCAGCTCGTGTCGTGAGATGTTGGGTTAAGTCCCGCAACGAGCGCAACCCCTGCCCCTAGTTGCCAGCGGGTCATGCCGGGCACTCTAGGGGGA CTGCCGGCGACAAGCCGGAGGAAGGTGGGGATGACGTCAAATCATCATGCCCCTTATGCCCTGGGCTACACACGTGCTACAATGGCCGGTACAAAGGGTTGCGAAC CCGCGAGGGGGAGCCAATCCCAAAAAGCCGGTCTCAGTTCGGATTGCAGGCTGCAACTCGCCTGCATGAAGGCGGAATCGCTAGTAATCGCGGATCAGCATGCCGC GGTGAATACGTTCCCGGGCCTTGTACACACCGCCCGTCACACCACGAGAGTCTGCAACACCCGAAGTCGGTGCGCCAACCCCTCACGGGGAGGCAGCCGCCGAAGG TGGGGCAGATGATTGGGGTGAAGTCGTAACAAGGTAA
18	Chloroflexi	ACGCAACACGAAGAACCTTACCCGGACTTGACATGGTGCTGCATCCCCTGGAAACAGGGGCGCCTTTGAGGGTGCACCACAGGTGCTGCATGGCTGTCGTCAGCTCG TGTCGTGAGATGTTGGGTTCAGTCCCGCAACGAGCGCAACCCGTGTCGGTAGTTACAGGTGTCTACCGAGACTGCCGCCGTGACCGGCGGAGGAAGGCGCGGATGA CGTCAAGTCAGCATGGCCCTTACGTCCGGGGCGACACACACGCTACAATGGCCACGACAATGCGTTGCCAAGCCGCAAGGTGGAGCTAATCGCCTAAACGTGGTCTC AGTGCAGATCGGGGGCTGCAACTCGCCCCCGTGAAGGCGGAGTTGCTAGTAACCGCGTATCAGCCATGGCGCGGTGAATACGTTCCCGGGCCTTGTACACACCGCCC GTCACGTCATGGGAGTGGCCAATGCTTGAAGTCCGTGTGCTAACCCCAGTCGGGGAGGCAGCGGCCGAGGGCAGGGGCCGCGACTGGGACGAAGTCGTAACAAGG TAGCCGTACCGGAAGGTGCGGCTGGATCACCTCCTTT
19	Chrysiogenetes	TACCTGGTCTTGACATCCCGATGCCGTATTCAGAGATGTATATTTCCCTTCGGGGACATCGGTGACAGGTGCTGCATGGCTGTCGTCAGCTCGCGTCGTGAGATGTTG GGTTAAGTCCCGCAACGAGCGCAACCCCTGCCATTAGTTGCCATCATTAAGTTGGGCACTCTAGTGGGACAGCCGGAGTAATCCGGAGGAAGGTGGGGACGACGTC AAGTCATCATGGCCCTTATGACCAGGGCTACACACGTGCTACAATGGCAAGGACAACGGGATGCGACCTCGCGAGAGTGAGCCAACCTCAAAAACCTTGTCTTAGTT CGGATTGCAGTCTGCAACTCGACTGCATGAAGTCGGAATCGCTAGTAATCGCAGGTCAGCATACTGCGGTGAATACGTTCCCGGGCCTTGTACACACCGCCCGTCACA CCACGAAAGTCGGTTTTGCCAGAAGCGGGTGACCGAATCTTCGGATAGGAGCCTTCGAAGGCAGGACTGGTGATTGGGGTGAAGTCGTAACAAGGTAGCCGTATCG GAAGGTGCGGCTGGATCACCTCCTTA
20	Bacteroidetes	CGAGGAACCTTACCCGGGCTTAAATTGCAGTGGAATGATGTGGAAACATGTCAGTGAGCAATCACCGCTGTGAAGGTGCTGCATGGTTGTCGTCAGCTCGTGCCGTG AGGTGTCGGCTTAAGTGCCATAACGAGCGCAACCCTTATCTTTAGTTACTAACAGGTTATGCTGAGGACTCTAGAGAGACTGCCGTCGTAAGATGTGAGGAAGGTGG GGATGACGTCAAATCAGCACGGCCCTTACGTCCGGGGCTACACACGTGTTACAATGGGGGGTACAGAAGGCAGCTAGCGGGTGACCGTATGCTAATCCCAAAATCC TCTCTCAGTTCGGATCGAAGTCTGCAACCCGACTTCGTGAAGCTGGATTCGCTAGTAATCGCGCATCAGCCACGGCGCGGTGAATACGTTCCCGGGCCTTGTACACAC CGCCCGTCAAGCCATGGGAGCCGGGGGTACCTGAAGTACGTAACCGCAAGGATCGTCCTAGGGTAAAACTGGTGACTGGGGCTAAGTCGTAACAAGGTAGCCGTAC CGGAAGGTGCGGCTGGAACACCTCCTTT

21	Aquificae	AGGGTTTGACATGCGGTGTGTCGGGTATGAAAGTACCCTAGGCTATGATTATTCATAGCCGCGCCGCACAGGTGGTGCATGGTCGTCGTCAGCTCGTGTCGTGAGAT GTTGGGTTAAGTCCCGCAACGAGCGCAACCCTTGCCCTGTGTTACCAGCGGGTAAAGCCGGGTACTCACAGGGGACTGCCGGCGATAAGTCGGAGGAAGGAGGGG ATGACGTCAGATCAGTATGCCCTTTATGCCCTGGGCTACACAGGCGCTACAGTGGCAGGGACAATGGGACGCAACGCAGCAATGCGGAGCAAATCCCCTAAACCCTG TCGTGGTGCGGATTGGGGGTTGCAACTCACCCCCATGAAGGCGGAATCGGTAGTAATGGCGAATCAGCAATGTCGCCGTGAATACGTTCCCGGGTCTTGTACACACC GCCCGTCACGCCATGGGAGTCGGGTTCATCGGAAGTCCCCGAGCTAACCCGCAAGGGAGGCAGGGGCCGATGATGGGCCTGATGACTGGGGCGAAGTCGTAACAA GGTAGCCCTAGGGGAACCTGGGGCTGGATCACCT
22	Caldiserica	GGTTTAATTCGATGCTACACGAAGAACCTTACCTGGGCTTGACATGCATGTGAAAGCCTGAAGAAACTCGGGCCCCCATAGGGGTTACACCCTATGGCACATGCACA GGTGCTGCATGGTTGTCGTCAGCTCGTGTCGTGAGATGTACGGTTAAGTCCGTGAACGAGCGCAACCCCTGCCCTTAGTTGCTAATAGGCTTCGGCCTATGCACTCTA AGGGGACTGCCAGCGATAAGCTGGAGGAAGGTGGGGATGACGTCAAATCCTCATGGCCCTTATGCCCAGGGCTACACACATGCGACAATGGTCGGGACAATGCGTT GCAAACCAGTAATGGGGAGCTAATCGCAAAAAACCGACCCCAGTACGGATTGAGGGTTGCAACTCACCCTCATGAAGCTGGAGTTGCTAGTAACCGCCGGTCAGCTA TACGGCGATGAATACGTTCCCGGGTCTTGTACACACCGCCCGTCACACCACCCGAGTTGCGTGCACCCGAAGTGGCTCGGTGAGTCACGAAGGTGTGCGTGATGAGG AGGGTGAAGTCGTAACAAGGTAGGTGTACGAGA
23	Thermotogae	TGGATGCTAAGCCAAGAACCTTACCAGGGCTTGACATGCCGGTGGTACCTCCCCGAAAGGGGTAGGGACCCAGTCCTTTGGGACTGGGAGCCGGCACAGGTGGTGC ACGGCCGTCGTCAGCTCGTGCCGTGAGGTGTTGGGTTAAGTCCCGCAACGAGCGCAACCCCTGCCCCTAGTTGCCAGCGGTTCGGCCGGGCACTCTAGGGGGACTG CCGGCGACGAGCCGGAGGAAGGAGGGGATGACGTCAGGTACTCGTGCCCCTTATGCCCTGGGCGACACACGCGCTACAATGGGCGGTACAATGGGTTGCGACCCC GCGAGGGGGAGCCAATCCCCAAAACCGCCCTCAGTTCGGATCGCAGGCTGCAACCCGCCTGCGTGAAGCCGGAATCGCTAGTAATCGCGGATCAGCCACGCCGCGG TGAATACGTTCCCGGGCCTTGTACACACCGCCCGTCACGCCACCCGAGTCGGGGGCTCCCGAAGACACCTGCCCCAACCCGAAAGGGAGGGGGGGTGTTGAGGGAG AACCTGGTGAGGGGGGCGAAGTCGTAACAAGGTAGCCGTAC
24	Tenericutes	CGAAAAACCTTACCTAGACTTGACATCCTTGGCAAAACTATAGAAATATAGTCGAGGTTAACCGAGAGACAGGTGGTGCATGGTTGTCGTCAGCTCGTGTCGTGAGA TGTTGGGTTAAGTCCCGCAACGAGCGCAACCCTTATCGTTAGTTACTTTGTCTAACGAGACTGCCAACGCAAGTTGGAGGAAGGTGGGGATGACGTCAAATCATCAT GCCCCTTATGTCTAGGGCTGCAAACGTGCTACAATGGCCAATACAAACAGTTACCAAACCGTAAGGTGGAGTTAATCTGCAAAGTTGGTCTCAGTTCGGATTGAGGG CTGCAATTCGCCCTCATGAAGTCGGAATCACTAGTAATCGCGAATCAGCTATGTCGCGGTGAATACGTTCTCGGGTCTTGTACACACCGCCCGTCAAACTACGAGAGT TGAGATTAATGATTGGAGTTAAGTCGTAACAAGGTACCCCTACGAGAACGTGGGGGTGGATCACCTCCTTTC
25	Nitrospirae	AGCGGTGGTGCATGTGGTTTAATTCGACGCAACGCGAGGAACCTTACCTAGGCTTGACATGTGGTGAGTAGCGAACCGAAAGGGGAGCGACCCGTCAAATCGGGCC ATCACACAGGTGCTGCATGGCTGTCGTCAGCTCGTGCCGTGAGGTGTTGGGTTCAGTCCCGCAACGAGCGCAACCCTCGCCCTTTGTTGCCATCGGGTAAAGCCGGG CACTCTAAGGGGACTGCCAGCGACAAGTTGGAGGAAGGAGAGGATGACGTCAAGTCATCATGGCCTTTATGCCTAGGGCCACACACGTGCAACAATGGCCGGTACA GACGGAGGCAATGCCGAGAGGCGGAGCAAACCCGAGAAAACCGGTCCCAGTTCGGATTGAGGTCTGCAACTCGACCTCATGAAGTCGGAATCGCTAGTAATCGCAT ATCAGAACGATGCGGTGAATACGTTCCCGGGCCTTGTACACACCGCCCGTCACACCACGAAAGTTTGTTGTACCCGAAGTCGGTGCCTTAACCTCGCAAGAGGAGAG AGCCGCCCAAGGTATGGCCGATGATTGGCGTG
26	Lentisphaerae	ATTCGAGGCAACGCGAAGAACCTTACCCGGGTTTGACATTGAGCGACGTTCGGTGAAAGTCGAATTCCCTTCGGGGCGCAAAAACAGGTGCTGCATGGCTGTCGTCA GCTTACTTGCTAACAGGTAATGCTGAGAACCTTAAGGAGACTGCCCGTGTTAAGCGGGAGGAAGGTGTGGACGACGTCAAGTCAGTATGGCCCTTACACCCGGGGC TGCACACCGTGCTACAATGGCCGGTACAAAGGGCAGCGACATAGTGATATGGAGCGAATCCCCAAAACCGGTCTCAGTACGGATTGGAGTCTGCAACTCGACTCCAT GAAGATGGAATCGCTAGTAAATGGGCATCAGCTACGGCTCATTGAATACGTTCCCGGGCCTTGTACACACCGCCCGTCACATCATGGGAGCTGAGTTCACCCGAAGT CGTTGCGCCAACCTGCTTACAGGAGGCAGACGCCGAAGGTGGGCTTAGTGACTGGGATGAAGTCGTAACAAGGTAGCC
27	Chlamydiae	TTCGATGCAACGCGAAGGACCTTACCTGGGTTTGACATGCATATGACCGCGGCAGAAATGTCGTTTTCCGCAAGGACATATGCACAGGTGCTGCATGGCTGTCGTCA GCTCGTGCCGTGAGGTGTTGGGTTAAGTCCCGCAACGAGCGCAACCCTTATCGTTAGTTGCCAGCACTTAGGGTGGGAACTCTAACGAGACTGCCTGGGTTAACCAG GAGGAAGGCGAGGATGACGTCAAGTCAGCATGGCCCTTATGCCCAGGGCGACACACGTGCTACAATGGCCAGTACAGAAGGTAGCAAGATCGTGAGATGGAGCAA ATCCTTAAAGCTGGCCCCAGTTCGGATTGTAGTCTGCAACTCGACTACATGAAGTCGGAATTGCTAGTAATGGCGTGTCAGCCATAACGCCGTGAATACGTTCCCGGG CCTTGTACACACCGCCCGTCACATCATGGGAGTTGGTTTTACCTTAAGTCGTTGACTCAACCCGCGAGGGGGAGAGGCGCCCAAGGTGAGGCTGATGACTAGGATGA AGTCGTAACAAGGTAGCCCTACCGGAAGGTGGG
28	Planctomycetes	AAACCTTATCCCAGGCTTGACATGCACGGATTAGCCGGCGGAAACGTCGGTGAGGCCGCAAGGAACAACGTGCACAGGTGCTGCATGGCTGTCGTCAGCTCGTGCC GTGAGGTGTTGGGTTAAGTCCCCTAACGAGCGAAACCCCTGTGTCTAGTTGCCAGCGGGTAAAGCCGGGAACTCTAGACAGACCGCCGGCGTTAAGCCGGAGGAAG GCGGGGATGACGTCAAGTCCTCATGGCCCTTATGCTTGGGGCTGCACACGTACTACAATGGGGCGGACAGAGCGTTGCTAGGCTGCAAAGTCATGCTAATCGCAAA AACCGTTCCTCAGTTCGGATTGCGGGCTGCAACCCGCCCGCATGAAGCTGGAATCGCTAGTAATCGCGGATCAGCATGCCGCGGTGAATGTGTTCCTGAGCCTTGTA CACACCGCCCGTCAAGCCACCAAAGCGGGGGGCATCCGAAGTCGCCGGAGCCGCAAGGCAGGCGCCGAAGATGAAACCCGTGATGGGGACTAAGTCGTAACAAGG TAACCGTAGGGGAACCTGCGGTTGGATCACCTCCTTT
29	Deferribacteres	GATGCTAACCGAAGAACCTTACCTGGGCTTGACATCCCCGGGACCTGCCAGAGATGGTGGGGTGCCTGGTTTTACCAGGAGCCGGGAGACAGGTGCTGCATGGCTG TCGTCAGCTCGTGCCGTGAGGTGTTGGGTTAAGTCCCGCAACGAGCGCAACCCCTACCCTTAGTTGCCATCGGTTAGGCCGGGCACTCTAAGGGGACTGCCCCGGAT AACGGGGAGGAAGGTGGGGATGACGTCAAGTCATCATGGCCCTTATGTCCAGGGCTACACACGTGCTACAATGGGGCGTACAGAGGGCAGCGAAGCCGCGAGGCT GAGCGAATCTCAGAAAGCGCTCCTCAGTTCGGATCGCAGTCTGCAACTCGACTGCGTGAAGCCGGAATCGCTAGTAATCGCAGGTCAGCAAAACTGCGGTGAATACG TTCCCGGGCCTTGTACACACCGCCCGTCACACCACGGGAGTTGGCTATACCTGAAGCCGGTGGCCCAACCCAGGCAACTGGGGGGGAGCCGTCCATGGTATGGCTG GCGACTGGGGTGAAGTCGTAACAAGGTAGCCGTA
30	Cyanobacteria	TACCAGGGTTTGACATCCTGAGAACCTCTTAGAAATTAGAGGGTGCCTTCGGGAATTCAGTGACAGGTGGTGCATGGCTGTCGTCAGCTCGTGTCGTGAGATGTTGG GTTAAGTCCCGCAACGAGCGCAACCCACGTTTTTAGTTGCCAGCATTTAGTTGGGCACTCTAGAAAGACCGCCGGTGATAAACCGGAGGAAGGTGTGGATGACGTCA AGTCATCATGCCCCTTACACCCTGGGCTACACACGTACTACAATGCTACGGACAAAGGGCAGCAAACTCGCGAGAGCTAGCAAATCCCATAAACCGTGGCTCAGTTCA GATCGTAGGCTGCAACTCGCCTACGTGAAGTAGGAATCGCTAGTAATCGCAGGTCAGCATACTGCGGTGAATACGTTCCCGGGCCTTGTACACACCGCCCGTCACAC CATGGAAGTTGGCCATGCCCGAAGTCGTTACTCCAACCCTTGTGGAGGAGGACGCCGAAGGTGGGGCTAATGACTGGGGTGAAGTCGTAACAAGGTAGCCGTACCG GAAGGTGCGGCTGGATCACCTCCTAA
31	Fusobacteria	CCTTACCAGCGTTTGACATCTTAGGAATGAGACAGAGATGTTTCAGTGTCCCTTCGGGGAAACCTAAAGACAGGTGGTGCATGGCTGTCGTCAGCTCGTGTCGTGAG ATGTTGGGTTAAGTCCCGCAACGAGCGCAACCCCTTTCGTATGTTACCATCATTAAGTTGGGGACTCATGCGATACTGCCTACGATGAGTAGGAGGAAGGTGGGGAT GACGTCAAGTCATCATGCCCCTTATACGCTGGGCTACACACGTGCTACAATGGGTAGAACAGAGAGTCGCAAAGCTGTGAAGTGGAGCTAATCTCAGAAAACTATTC TTAGTTCGGATTGTACTCTGCAACTCGAGTACATGAAGTTGGAATCGCTAGTAATCGCGAATCAGCAATGTCGCGGTGAATACGTTCTCGGGTCTTGTACACACCGCC CGTCACACCACGAGAGTTGGTTGCACAAGAAGTAGCAGGCCTAACCGTAAGGAGGGGATGCTCCGAGGGTGTGATTAGCGATTGGGGTGAAGTCGTAACAAGGTATC CGTACGGGAACGTGCGGCTGGATC

Supplementary Table 2: Primer sequences for LAMP

Primer set number	Primer name	Nucleotide sequence
1	lamp_16s_1_F3	TTGGGGTCTGCAACTCGA
	lamp_16s_1_B3	ATCGCCGATCCCACCTTC
	lamp_16s_1_FIP	CCGGGAACGTATTCACCGCAGTTTTTTCCATGAAGTCGGAGTCGC
	lamp_16s_1_BIP	CTTGTACACACCGCCCGTCATTTTTTTCCCTCCACAAGGGTTAGG
2	lamp_16s_2_F3	TGACGTCAAATCCTCATGGC
	lamp_16s_2_B3	GTCCGGGAACGTATTCACC
	lamp_16s_2_FIP	TAGCTCCCCCTCGCGAGTTGTTTTTTATGTCTAGGGCAACACACG
	lamp_16s_2_BIP	ATCCGGTCCCAGTTCGGATTGTTTTTTTCCGCGATTACTAGCGATTC
3	lamp_16s_3_F3	CAATGGCCAGCACAGAGG
	lamp_16s_3_B3	ACTCGGGTGGTGTGACG
	lamp_16s_3_FIP	TCGAGTTGCAGACTGCAATCCGTTTTTTCAAGTCCGCGAGGACAAGC
	lamp_16s_3_BIP	GCATGAAGCCGGAATCGCTAGTTTTTTTTGGCGGTGTGTACAAGGC
4	lamp_16s_4_F3	CGAAGAACCTTACCAGGGC
	lamp_16s_4_B3	CTGGCAACTAAGGGCAGG
	lamp_16s_4_FIP	GCTCCAAATAGGGGAAACCCCCTTTTTTGACATGCAGGCTGTAAGCT
	lamp_16s_4_BIP	CACAGGTGGTGCATGGCTGTTTTTTTTTGCGGGACTTAACCCAAC
5	lamp_16s_5_F3	TGTTGGGTTAAGTCCCGCA
	lamp_16s_5_B3	GATTTGCTCCCCCTTACGG
	lamp_16s_5_FIP	TTCCTCCGGGTTGTCCCCGTTTTTTAACCCTTGCCCTTAGTTGCC
	lamp_16s_5_BIP	AGTCATCATGGCCCTTATGCCCTTTTTTCGCTTCCCTCTGTACCGC
6	lamp_16s_6_F3	TTGGGTTAAGTCCCGCAAC
	lamp_16s_6_B3	GGATTGGCTCCATCTCGC
	lamp_16s_6_FIP	CGTTATCCGCGGCAGTCTTCTGTTTTTTGCGCAACCCCTATTCTGTG
	lamp_16s_6_BIP	GAGGAAGGTGGGGATGACGTCATTTTTTGCCCTCTGTCTATGCCATTG
7	lamp_16s_7_F3	AGAACCTTACCTGGGCTTGA
	lamp_16s_7_B3	GGCCATGAGGACTTGACG
	lamp_16s_7_FIP	GACACGAGCTGACGACAGCCTTTTTTAAAGATGAGGTCCTTCGGGA
	lamp_16s_7_BIP	GCAACGAGCGCAACCCCTACTTTTTTCTACTTGCGTAGGCAGTTCA
8	lamp_16s_8_F3	CAACCCGCCTACACGAAG

	lamp_16s_8_B3	CGGCTACCTTGTTACGACTT
	lamp_16s_8_FIP	GGTGTGTACAAGACCCGGGAACTTTTTTATCGCTAGTAATGGCGCATC
	lamp_16s_8_BIP	GCCCGTCACATCATGGAAGCCTTTTTTAGTCTCACCTTAGGACCCTG
9	lamp_16s_9_F3	GGCCCAGTTCGGATTGG
	lamp_16s_9_B3	ACCTTGTTACGACTTCGCC
	lamp_16s_9_FIP	GGAACGTATTCACCGCGGCATGTTTTTTGACCCCATGAAGCCGGAAT
	lamp_16s_9_BIP	ATGGGAGCGGGCTCTACCCTTTTTTTCACGGGCCCTACCCT
10	lamp_16s_10_F3	GCATCCTCAGTTCGGATTGG
	lamp_16s_10_B3	TGTTACGACTTAGCCCCAGT
	lamp_16s_10_FIP	GTATTCACCGCGCCGTGCTGTTTTTTTCTGCAACCCGACTCCAT
	lamp_16s_10_BIP	CGGGGGTACCCGAAGTCAGTTTTTTTTTTTACCTTCGGCAGCTCC
11	lamp_16s_11_F3	ACGTCTGGGGCTACACAC
	lamp_16s_11_B3	CAGCTTCCATGGCGTGAC
	lamp_16s_11_FIP	CCGGCTTTAGGGATTGGCTCCTTTTTTGTGCTACAATGGCCGGTAC
	lamp_16s_11_BIP	GTCTGCAACTCGACGGCATGATTTTTTGCCCGGGAACGTATTCAC
12	lamp_16s_12_F3	TCCGGATTGGAGTCTGCA
	lamp_16s_12_B3	CACCCCAGTCATGAATCACA
	lamp_16s_12_FIP	GCCCGGGAACGTATTCACCGTTTTTTTCGACTCCATGAAGTCGGAA
	lamp_16s_12_BIP	CTTGTACACACCGCCCGTCATTTTTTCTCCCGAAGGTTAAGCTACC
13	lamp_16s_13_F3	AAAACCGTTCTCAGTTCGGA
	lamp_16s_13_B3	CCCAATCATCTGTCCCACC
	lamp_16s_13_FIP	ATTCACCGCGGCATGCTGATCTTTTTTCTGCAACTCGCCTACATGA
	lamp_16s_13_BIP	ACGTTCCCGGGCCTTGTACATTTTTTCCAAAAAGGTTACCCCACCG
14	lamp_16s_14_F3	CAACGTTCCGCACAGGTG
	lamp_16s_14_B3	ACGTGTGTAGCCCAGGAT
	lamp_16s_14_FIP	TGGAAACGTGGGTTGCGCTCTTTTTTGTCAGCTCGTGTCGTGAG
	lamp_16s_14_BIP	GGAGAGACTGCCGGGGACAATTTTTTAGGGCCATGAGGACTTGA
15	lamp_16s_15_F3	GAGCACTCTGGCGAAACC
	lamp_16s_15_B3	CTTCATGGAGTCGAGTTGCA
	lamp_16s_15_FIP	GCACGTGTGTAGCCCTGGACTTTTTTGGAGGAAGGTGGGGATGA
	lamp_16s_15_BIP	AATGGCCGGTACAAACCGCTTTTTTTCTCCAATCCGAACTGAGGC

16	lamp_16s_16_F3	TTAAGTCCCGCAACGAGC
	lamp_16s_16_B3	CTCGCGGTTTCGCAACTC
	lamp_16s_16_FIP	ATCGCCGGCAGTCCCTCTAGTTTTTTAACCCCTGCCTCTAGTTACC
	lamp_16s_16_BIP	AAGCTGGAGGAAGGTGGGGATTTTTTTGTACCGGCCATTGTAGCAC
17	lamp_16s_17_F3	ACATCCCGCTGACCGC
	lamp_16s_17_B3	TTGTCGCCGGCAGTCC
	lamp_16s_17_FIP	GACGACAACCATGCACCACCTTTTTTTCAGAGATGGGGCTTCCCT
	lamp_16s_17_BIP	TGTTGGGTTAAGTCCCGCAACGTTTTTTAGTGCCCGGCATGACC
18	lamp_16s_18_F3	AGAACCTTACCCGGACTTGA
	lamp_16s_18_B3	TTCCTCCGCCGGTCAC
	lamp_16s_18_FIP	CATGCAGCACCTGTGGTGCACTTTTTTCATGGTGCTGCATCCCCT
	lamp_16s_18_BIP	TGAGATGTTGGGTTCAGTCCCGTTTTTTCGGCAGTCTCGGTAGACAC
19	lamp_16s_19_F3	TGAGCCAACCTCAAAAACCT
	lamp_16s_19_B3	TGCCTTCGAAGGCTCCTA
	lamp_16s_19_FIP	CGCAGTATGCTGACCTGCGATTTTTTTTCGGATTGCAGTCTGCAACTC
	lamp_16s_19_BIP	GTGAATACGTTCCCGGGCCTTTTTTTATTCGGTCACCCGCTTCT
20	lamp_16s_20_F3	AGAGAGACTGCCGTCGTAAG
	lamp_16s_20_B3	TCACGAAGTCGGGTTGCA
	lamp_16s_20_FIP	CGTGTGTAGCCCCGGACGTATTTTTTTGTGAGGAAGGTGGGGATG
	lamp_16s_20_BIP	ACAATGGGGGGTACAGAAGGCTTTTTTCGATCCGAACTGAGAGAGGA
21	lamp_16s_21_F3	CACAGGTGGTGCATGGTC
	lamp_16s_21_B3	CTGTAGCGCCTGTGTAGC
	lamp_16s_21_FIP	AACACAGGGCAAGGGTTGCGTTTTTTGTCAGCTCGTGTCGTGAG
	lamp_16s_21_BIP	GGACTGCCGGCGATAAGTCGTTTTTTCCAGGGCATAAAGGGCATAC
22	lamp_16s_22_F3	TGCACTCTAAGGGGACTGC
	lamp_16s_22_B3	CAGCTTCATGAGGGTGAGTT
	lamp_16s_22_FIP	CGCATGTGTGTAGCCCTGGGTTTTTTCTGGAGGAAGGTGGGGAT
	lamp_16s_22_BIP	CAATGGTCGGGACAATGCGTTGTTTTTTGCAACCCTCAATCCGTACTG
23	lamp_16s_23_F3	GCACTCTAGGGGGACTGC
	lamp_16s_23_B3	CTAGCGATTCCGGCTTCAC
	lamp_16s_23_FIP	TAGCGCGTGTGTCGCCCAGTTTTTTGAGGAAGGAGGGGATGACG

	lamp_16s_23_BIP	ATGGGCGGTACAATGGGTTGCTTTTTTCCTGCGATCCGAACTGAGG
24	lamp_16s_24_F3	ATTCGCCCTCATGAAGTCG
	lamp_16s_24_B3	ATCCACCCCCACGTTCTC
	lamp_16s_24_FIP	TGACGGGCGGTGTGTACAAGTTTTTTATCGCGAATCAGCTATGTCG
	lamp_16s_24_BIP	ACCGTGTTGCTAACCGCAAGGTTTTTTAGGGGTACCTTGTTACGACT
25	lamp_16s_25_F3	AAGCCGGGCACTCTAAGG
	lamp_16s_25_B3	CTTCATGAGGTCGAGTTGCA
	lamp_16s_25_FIP	GCCCTAGGCATAAAGGCCATGATTTTTTGACTGCCAGCGACAAGTT
	lamp_16s_25_BIP	AACAATGGCCGGTACAGACGGTTTTTTCCTCAATCCGAACTGGGAC
26	lamp_16s_26_F3	CCTTACCCGGGTTTGACATT
	lamp_16s_26_B3	TCGTCCACACCTTCCTCC
	lamp_16s_26_FIP	CAGCCATGCAGCACCTGTTTTTTTTTTGAGCGACGTTCGGTGAAAG
	lamp_16s_26_BIP	TTAAGTCCGGCAACGAGCGCTTTTTTAACACGGGCAGTCTCCTT
27	lamp_16s_27_F3	TGACATGCATATGACCGCG
	lamp_16s_27_B3	ATGCTGACTTGACGTCATCC
	lamp_16s_27_FIP	CAACACCTCACGGCACGAGCTTTTTTAAATGTCGTTTTCCGCAAGG
	lamp_16s_27_BIP	GTTGCCAGCACTTAGGGTGGGTTTTTTTCGCCTTCCTCCTGGTTA
28	lamp_16s_28_F3	AGCGAAACCCCTGTGTCT
	lamp_16s_28_B3	TGAGGAACGGTTTTTGCGAT
	lamp_16s_28_FIP	ACTTGACGTCATCCCCGCCTTTTTTTGGGTAAAGCCGGGAACTCT
	lamp_16s_28_BIP	CCTCATGGCCCTTATGCTTGGGTTTTTTAGCCTAGCAACGCTCTGT
29	lamp_16s_29_F3	CAGTTCGGATCGCAGTCTG
	lamp_16s_29_B3	CCAGCCATACCATGGACG
	lamp_16s_29_FIP	CGGGAACGTATTCACCGCAGTTTTTTTTGACTGCGTGAAGCCGGAAT
	lamp_16s_29_BIP	GCCTTGTACACACCGCCCGTTTTTTTTCCCCCCCAGTTGCCT
30	lamp_16s_30_F3	ACAAAGGGCAGCAAACTCG
	lamp_16s_30_B3	CATTAGCCCCACCTTCGG
	lamp_16s_30_FIP	TGCTGACCTGCGATTACTAGCGTTTTTTCCCATAAACCGTGGCTCAG
	lamp_16s_30_BIP	GTGAATACGTTCCCGGGCCTTTTTTTGGGTTGGAGTAACGACTTCG
31	lamp_16s_31_F3	AAAGACAGGTGGTGCATGG
	lamp_16s_31_B3	GCTTTGCGACTCTCTGTTCT

	lamp_16s_31_FIP	ACATACGAAAGGGGTTGCGCTCTTTTTTGTCAGCTCGTGTCGTGAGA
	lamp_16s_31_BIP	TAGGAGGAAGGTGGGGATGACGTTTTTTTTGTAGCACGTGTGTAGCC

Supplementary Table 3: Length of oligomers and the number of bases in APC

Length (lt)	Allowed margin bases(mg)	Allowed mismatched bases(mt)	Acceptable homologous positions between target homologies (sr)	Number of APC
6	0, 1, 2 or 3	0	1, 2, 3, 5, 7 or 9	24
7		0 or 1		48
8		0 or 1		48
9		0, 1, 2 or 3		96
10		0, 1, 2 or 3		96
11		0, 1, 2, 3 or 4		120
12		0, 1, 2, 3, 4 or 5		144
13		0, 1, 2, 3, 4 or 5		144
14		0, 1, 2, 3, 4 or 5		144
15		0, 1, 2, 3, 4 or 5		144
16		0, 1, 2, 3, 4, 5 or 6		168
17		0, 1, 2, 3, 4, 5 or 6		168
18		0, 1, 2, 3, 4, 5 or 6		168
Total Number of APC				1512

Legend: Configuration of oligomer base length (ln), margin (mg), allowable number of mismatched bases (mt) when determining alignment, and allowable number of incorrect positions on alignment (sr) when configuring APC. The allowable number of incorrect positions in the margin and alignment arrangement is set independently of the oligomer base length, but the allowable number of mismatched bases at the time of alignment determination is set depending on the oligomer base length.

Supplementary Table 4: Homologous character transformation

LAMP Primer	Direction of homology	Character for
F1c	+	A
F1c	—	B
F2	+	C
F2	—	D
F3	+	E
F3	—	F
B1c	+	G
B1c	—	H
B2	+	I
B2	—	J
B3	+	K
B3	—	L

Legend: Alphabet settings for each priming region and alignment direction to determine the allowable number of mismatches in alignment during amplification determination by character string calculation.

Supplementary Table 5: Clusters of APC according to their predictions

cluster number	APC
1	mg0_ln10_mt0_sr7; mg0_ln10_mt0_sr9; mg0_ln11_mt0_sr7; mg0_ln11_mt0_sr5; mg0_ln11_mt0_sr3; mg0_ln11_mt0_sr9; mg0_ln11_mt0_sr1; mg0_ln11_mt0_sr2; mg0_ln12_mt0_sr7; mg0_ln12_mt0_sr5; mg0_ln12_mt0_sr3; mg0_ln12_mt0_sr9; mg0_ln12_mt0_sr1; mg0_ln12_mt0_sr2; mg0_ln13_mt0_sr7; mg0_ln13_mt0_sr5; mg0_ln13_mt0_sr3; mg0_ln13_mt0_sr9; mg0_ln13_mt0_sr1; mg0_ln13_mt0_sr2; mg0_ln13_mt1_sr7; mg0_ln13_mt1_sr5; mg0_ln13_mt1_sr3; mg0_ln13_mt1_sr9; mg0_ln13_mt1_sr1; mg0_ln13_mt1_sr2; mg0_ln14_mt0_sr7; mg0_ln14_mt0_sr5; mg0_ln14_mt0_sr3; mg0_ln14_mt0_sr9; mg0_ln14_mt0_sr1; mg0_ln14_mt0_sr2; mg0_ln14_mt1_sr7; mg0_ln14_mt1_sr5; mg0_ln14_mt1_sr3; mg0_ln14_mt1_sr9; mg0_ln14_mt1_sr1; mg0_ln14_mt1_sr2; mg0_ln15_mt0_sr7; mg0_ln15_mt0_sr5; mg0_ln15_mt0_sr3; mg0_ln15_mt0_sr9; mg0_ln15_mt0_sr1; mg0_ln15_mt0_sr2; mg0_ln15_mt1_sr7; mg0_ln15_mt1_sr5; mg0_ln15_mt1_sr3; mg0_ln15_mt1_sr9; mg0_ln15_mt1_sr1; mg0_ln15_mt1_sr2; mg0_ln16_mt0_sr7; mg0_ln16_mt0_sr5; mg0_ln16_mt0_sr3; mg0_ln16_mt0_sr9; mg0_ln16_mt0_sr1; mg0_ln16_mt0_sr2; mg0_ln16_mt1_sr7; mg0_ln16_mt1_sr5; mg0_ln16_mt1_sr3; mg0_ln16_mt1_sr9; mg0_ln16_mt1_sr1; mg0_ln16_mt1_sr2; mg0_ln17_mt0_sr7; mg0_ln17_mt0_sr5; mg0_ln17_mt0_sr3; mg0_ln17_mt0_sr9; mg0_ln17_mt0_sr1; mg0_ln17_mt0_sr2; mg0_ln17_mt1_sr7; mg0_ln17_mt1_sr5; mg0_ln17_mt1_sr3; mg0_ln17_mt1_sr9; mg0_ln17_mt1_sr1; mg0_ln17_mt1_sr2; mg0_ln18_mt0_sr7; mg0_ln18_mt0_sr5; mg0_ln18_mt0_sr3; mg0_ln18_mt0_sr9; mg0_ln18_mt0_sr1; mg0_ln18_mt0_sr2; mg0_ln18_mt1_sr7; mg0_ln18_mt1_sr5; mg0_ln18_mt1_sr3; mg0_ln18_mt1_sr9; mg0_ln18_mt1_sr1; mg0_ln18_mt1_sr2; mg0_ln7_mt0_sr7; mg0_ln7_mt0_sr5; mg0_ln7_mt0_sr3; mg0_ln7_mt0_sr9; mg0_ln7_mt0_sr1; mg0_ln7_mt0_sr2; mg0_ln8_mt0_sr7; mg0_ln8_mt0_sr5; mg0_ln8_mt0_sr3; mg0_ln8_mt0_sr9; mg0_ln8_mt0_sr1; mg0_ln8_mt0_sr2; mg0_ln9_mt0_sr7; mg0_ln9_mt0_sr5; mg0_ln9_mt0_sr3; mg0_ln9_mt0_sr9; mg0_ln9_mt0_sr1; mg0_ln9_mt0_sr2; mg1_ln10_mt0_sr7; mg1_ln10_mt0_sr5; mg1_ln10_mt0_sr3; mg1_ln10_mt0_sr9; mg1_ln10_mt0_sr1; mg1_ln10_mt0_sr2; mg1_ln11_mt0_sr7; mg1_ln11_mt0_sr5; mg1_ln11_mt0_sr3; mg1_ln11_mt0_sr9; mg1_ln11_mt0_sr1; mg1_ln11_mt0_sr2; mg1_ln12_mt0_sr7; mg1_ln12_mt0_sr5; mg1_ln12_mt0_sr3; mg1_ln12_mt0_sr9; mg1_ln12_mt0_sr1; mg1_ln12_mt0_sr2; mg1_ln12_mt1_sr7; mg1_ln12_mt1_sr5; mg1_ln12_mt1_sr3; mg1_ln12_mt1_sr9; mg1_ln12_mt1_sr1; mg1_ln12_mt1_sr2; mg1_ln13_mt0_sr7; mg1_ln13_mt0_sr5; mg1_ln13_mt0_sr3; mg1_ln13_mt0_sr9; mg1_ln13_mt0_sr1; mg1_ln13_mt0_sr2; mg1_ln13_mt1_sr7; mg1_ln13_mt1_sr5; mg1_ln13_mt1_sr3; mg1_ln13_mt1_sr9; mg1_ln13_mt1_sr1; mg1_ln13_mt1_sr2; mg1_ln14_mt0_sr7; mg1_ln14_mt0_sr5; mg1_ln14_mt0_sr3; mg1_ln14_mt0_sr9; mg1_ln14_mt0_sr1; mg1_ln14_mt0_sr2; mg1_ln14_mt1_sr7; mg1_ln14_mt1_sr5; mg1_ln14_mt1_sr3; mg1_ln14_mt1_sr9; mg1_ln14_mt1_sr1; mg1_ln14_mt1_sr2; mg1_ln15_mt0_sr7; mg1_ln15_mt0_sr5; mg1_ln15_mt0_sr3; mg1_ln15_mt0_sr9; mg1_ln15_mt0_sr1; mg1_ln15_mt0_sr2; mg1_ln15_mt1_sr7; mg1_ln15_mt1_sr5; mg1_ln15_mt1_sr3; mg1_ln15_mt1_sr9; mg1_ln15_mt1_sr1; mg1_ln15_mt1_sr2; mg1_ln16_mt0_sr7; mg1_ln16_mt0_sr5; mg1_ln16_mt0_sr3; mg1_ln16_mt0_sr9; mg1_ln16_mt0_sr1; mg1_ln16_mt0_sr2; mg1_ln16_mt1_sr7; mg1_ln16_mt1_sr5; mg1_ln16_mt1_sr3; mg1_ln16_mt1_sr9; mg1_ln16_mt1_sr1; mg1_ln16_mt1_sr2; mg1_ln17_mt0_sr7; mg1_ln17_mt0_sr5; mg1_ln17_mt0_sr3; mg1_ln17_mt0_sr9; mg1_ln17_mt0_sr1; mg1_ln17_mt0_sr2; mg1_ln17_mt1_sr7; mg1_ln17_mt1_sr5; mg1_ln17_mt1_sr3; mg1_ln17_mt1_sr9; mg1_ln17_mt1_sr1; mg1_ln17_mt1_sr2; mg1_ln18_mt1_sr7; mg1_ln18_mt1_sr5; mg1_ln18_mt1_sr3; mg1_ln18_mt1_sr9; mg1_ln18_mt1_sr1; mg1_ln18_mt1_sr2; mg1_ln6_mt0_sr7; mg1_ln6_mt0_sr5; mg1_ln6_mt0_sr3; mg1_ln6_mt0_sr9; mg1_ln6_mt0_sr1; mg1_ln6_mt0_sr2; mg1_ln7_mt0_sr7; mg1_ln7_mt0_sr5; mg1_ln7_mt0_sr3; mg1_ln7_mt0_sr9; mg1_ln7_mt0_sr1; mg1_ln7_mt0_sr2; mg1_ln8_mt0_sr7; mg1_ln8_mt0_sr5; mg1_ln8_mt0_sr3; mg1_ln8_mt0_sr9; mg1_ln8_mt0_sr1; mg1_ln8_mt0_sr2; mg1_ln9_mt0_sr7; mg1_ln9_mt0_sr5; mg1_ln9_mt0_sr3; mg1_ln9_mt0_sr9; mg1_ln9_mt0_sr1; mg1_ln9_mt0_sr2; mg2_ln10_mt0_sr7; mg2_ln10_mt0_sr5; mg2_ln10_mt0_sr3; mg2_ln10_mt0_sr9; mg2_ln10_mt0_sr1; mg2_ln10_mt0_sr2; mg2_ln11_mt0_sr7; mg2_ln11_mt0_sr5; mg2_ln11_mt0_sr3; mg2_ln11_mt0_sr9; mg2_ln11_mt0_sr1; mg2_ln11_mt0_sr2; mg2_ln11_mt1_sr7; mg2_ln11_mt1_sr5; mg2_ln11_mt1_sr3; mg2_ln11_mt1_sr9; mg2_ln11_mt1_sr1; mg2_ln11_mt1_sr2; mg2_ln12_mt0_sr7; mg2_ln12_mt0_sr5; mg2_ln12_mt0_sr3; mg2_ln12_mt0_sr9; mg2_ln12_mt0_sr1; mg2_ln12_mt0_sr2; mg2_ln12_mt1_sr7; mg2_ln12_mt1_sr5; mg2_ln12_mt1_sr3; mg2_ln12_mt1_sr9; mg2_ln12_mt1_sr1; mg2_ln12_mt1_sr2; mg2_ln13_mt0_sr7; mg2_ln13_mt0_sr5; mg2_ln13_mt0_sr3; mg2_ln13_mt0_sr9; mg2_ln13_mt0_sr1; mg2_ln13_mt0_sr2; mg2_ln13_mt1_sr7; mg2_ln13_mt1_sr5; mg2_ln13_mt1_sr3; mg2_ln13_mt1_sr9; mg2_ln13_mt1_sr1; mg2_ln13_mt1_sr2; mg2_ln14_mt0_sr7; mg2_ln14_mt0_sr5; mg2_ln14_mt0_sr3; mg2_ln14_mt0_sr9; mg2_ln14_mt0_sr1; mg2_ln14_mt0_sr2; mg2_ln14_mt1_sr7; mg2_ln14_mt1_sr5; mg2_ln14_mt1_sr3; mg2_ln14_mt1_sr9; mg2_ln14_mt1_sr1; mg2_ln14_mt1_sr2; mg2_ln15_mt0_sr7; mg2_ln15_mt0_sr5; mg2_ln15_mt0_sr3; mg2_ln15_mt0_sr9; mg2_ln15_mt0_sr1; mg2_ln15_mt0_sr2; mg2_ln15_mt1_sr7; mg2_ln15_mt1_sr5; mg2_ln15_mt1_sr3; mg2_ln15_mt1_sr9; mg2_ln15_mt1_sr1; mg2_ln15_mt1_sr2; mg2_ln16_mt0_sr7; mg2_ln16_mt0_sr5; mg2_ln16_mt0_sr3; mg2_ln16_mt0_sr9; mg2_ln16_mt0_sr1; mg2_ln16_mt0_sr2; mg2_ln16_mt1_sr7; mg2_ln16_mt1_sr5; mg2_ln16_mt1_sr3; mg2_ln16_mt1_sr9; mg2_ln16_mt1_sr1; mg2_ln16_mt1_sr2; mg2_ln17_mt1_sr7; mg2_ln17_mt1_sr5; mg2_ln17_mt1_sr3; mg2_ln17_mt1_sr9; mg2_ln17_mt1_sr1; mg2_ln17_mt1_sr2; mg2_ln18_mt2_sr7; mg2_ln18_mt2_sr5; mg2_ln18_mt2_sr3; mg2_ln18_mt2_sr9; mg2_ln18_mt2_sr1; mg2_ln18_mt2_sr2; mg2_ln6_mt0_sr3; mg2_ln6_mt0_sr1; mg2_ln6_mt0_sr2; mg2_ln7_mt0_sr7; mg2_ln7_mt0_sr5; mg2_ln7_mt0_sr3; mg2_ln7_mt0_sr9; mg2_ln7_mt0_sr1; mg2_ln7_mt0_sr2; mg2_ln8_mt0_sr7; mg2_ln8_mt0_sr5; mg2_ln8_mt0_sr3; mg2_ln8_mt0_sr9; mg2_ln8_mt0_sr1; mg2_ln8_mt0_sr2; mg2_ln9_mt0_sr7; mg2_ln9_mt0_sr5; mg2_ln9_mt0_sr3; mg2_ln9_mt0_sr9; mg2_ln9_mt0_sr1; mg2_ln9_mt0_sr2; mg3_ln10_mt0_sr7; mg3_ln10_mt0_sr5; mg3_ln10_mt0_sr3; mg3_ln10_mt0_sr9; mg3_ln10_mt0_sr1; mg3_ln10_mt0_sr2; mg3_ln10_mt1_sr7; mg3_ln10_mt1_sr5; mg3_ln10_mt1_sr3; mg3_ln10_mt1_sr9; mg3_ln10_mt1_sr1; mg3_ln10_mt1_sr2; mg3_ln11_mt0_sr7; mg3_ln11_mt0_sr5; mg3_ln11_mt0_sr3; mg3_ln11_mt0_sr9; mg3_ln11_mt0_sr1; mg3_ln11_mt0_sr2; mg3_ln11_mt1_sr7; mg3_ln11_mt1_sr5; mg3_ln11_mt1_sr3; mg3_ln11_mt1_sr9; mg3_ln11_mt1_sr1; mg3_ln11_mt1_sr2; mg3_ln12_mt0_sr7; mg3_ln12_mt0_sr5; mg3_ln12_mt0_sr3; mg3_ln12_mt0_sr9; mg3_ln12_mt0_sr1; mg3_ln12_mt0_sr2; mg3_ln12_mt1_sr7; mg3_ln12_mt1_sr5; mg3_ln12_mt1_sr3; mg3_ln12_mt1_sr9; mg3_ln12_mt1_sr1; mg3_ln12_mt1_sr2; mg3_ln13_mt0_sr7; mg3_ln13_mt0_sr5; mg3_ln13_mt0_sr3; mg3_ln13_mt0_sr9; mg3_ln13_mt0_sr1; mg3_ln13_mt0_sr2; mg3_ln13_mt1_sr7; mg3_ln13_mt1_sr5; mg3_ln13_mt1_sr3; mg3_ln13_mt1_sr9; mg3_ln13_mt1_sr1; mg3_ln13_mt1_sr2; mg3_ln14_mt0_sr7; mg3_ln14_mt0_sr5; mg3_ln14_mt0_sr3; mg3_ln14_mt0_sr9; mg3_ln14_mt0_sr1; mg3_ln14_mt0_sr2; mg3_ln14_mt1_sr7; mg3_ln14_mt1_sr5; mg3_ln14_mt1_sr3; mg3_ln14_mt1_sr9; mg3_ln14_mt1_sr1; mg3_ln14_mt1_sr2; mg3_ln15_mt0_sr7; mg3_ln15_mt0_sr5; mg3_ln15_mt0_sr3; mg3_ln15_mt0_sr9; mg3_ln15_mt0_sr1; mg3_ln15_mt0_sr2; mg3_ln15_mt1_sr7; mg3_ln15_mt1_sr5; mg3_ln15_mt1_sr3; mg3_ln15_mt1_sr9; mg3_ln15_mt1_sr1; mg3_ln15_mt1_sr2; mg3_ln16_mt1_sr7; mg3_ln16_mt1_sr5; mg3_ln16_mt1_sr3; mg3_ln16_mt1_sr9; mg3_ln16_mt1_sr1; mg3_ln16_mt1_sr2; mg3_ln6_mt0_sr3;

	mg3_ln6_mt0_sr1; mg3_ln6_mt0_sr2; mg3_ln7_mt0_sr7; mg3_ln7_mt0_sr5; mg3_ln7_mt0_sr3; mg3_ln7_mt0_sr9; mg3_ln7_mt0_sr1; mg3_ln7_mt0_sr2; mg3_ln8_mt0_sr7; mg3_ln8_mt0_sr5; mg3_ln8_mt0_sr3; mg3_ln8_mt0_sr9; mg3_ln8_mt0_sr1; mg3_ln8_mt0_sr2; mg3_ln9_mt0_sr7; mg3_ln9_mt0_sr5; mg3_ln9_mt0_sr3; mg3_ln9_mt0_sr9; mg3_ln9_mt0_sr1; mg3_ln9_mt0_sr2; mg0_ln10_mt0_sr5; mg0_ln10_mt0_sr3; mg0_ln10_mt0_sr1; mg0_ln10_mt0_sr2; mg2_ln6_mt0_sr7; mg2_ln6_mt0_sr9; mg2_ln6_mt0_sr5
2	mg0_ln10_mt1_sr7; mg0_ln10_mt1_sr9; mg0_ln11_mt1_sr7; mg0_ln11_mt1_sr5; mg0_ln11_mt1_sr3; mg0_ln11_mt1_sr9; mg0_ln11_mt1_sr1; mg0_ln11_mt1_sr2; mg0_ln12_mt1_sr7; mg0_ln12_mt1_sr5; mg0_ln12_mt1_sr3; mg0_ln12_mt1_sr9; mg0_ln12_mt1_sr1; mg0_ln12_mt1_sr2; mg0_ln14_mt2_sr7; mg0_ln14_mt2_sr5; mg0_ln14_mt2_sr3; mg0_ln14_mt2_sr9; mg0_ln14_mt2_sr1; mg0_ln14_mt2_sr2; mg0_ln15_mt2_sr7; mg0_ln15_mt2_sr5; mg0_ln15_mt2_sr3; mg0_ln15_mt2_sr9; mg0_ln15_mt2_sr1; mg0_ln15_mt2_sr2; mg0_ln16_mt2_sr7; mg0_ln16_mt2_sr5; mg0_ln16_mt2_sr3; mg0_ln16_mt2_sr9; mg0_ln16_mt2_sr1; mg0_ln16_mt2_sr2; mg0_ln17_mt2_sr7; mg0_ln17_mt2_sr5; mg0_ln17_mt2_sr3; mg0_ln17_mt2_sr9; mg0_ln17_mt2_sr1; mg0_ln17_mt2_sr2; mg0_ln18_mt2_sr7; mg0_ln18_mt2_sr5; mg0_ln18_mt2_sr3; mg0_ln18_mt2_sr9; mg0_ln18_mt2_sr1; mg0_ln18_mt2_sr2; mg1_ln10_mt1_sr7; mg1_ln10_mt1_sr5; mg1_ln10_mt1_sr3; mg1_ln10_mt1_sr9; mg1_ln10_mt1_sr1; mg1_ln10_mt1_sr2; mg1_ln11_mt1_sr7; mg1_ln11_mt1_sr5; mg1_ln11_mt1_sr3; mg1_ln11_mt1_sr9; mg1_ln11_mt1_sr1; mg1_ln11_mt1_sr2; mg1_ln14_mt2_sr7; mg1_ln14_mt2_sr5; mg1_ln14_mt2_sr3; mg1_ln14_mt2_sr9; mg1_ln14_mt2_sr1; mg1_ln14_mt2_sr2; mg1_ln15_mt2_sr7; mg1_ln15_mt2_sr5; mg1_ln15_mt2_sr3; mg1_ln15_mt2_sr9; mg1_ln15_mt2_sr1; mg1_ln15_mt2_sr2; mg1_ln16_mt2_sr7; mg1_ln16_mt2_sr5; mg1_ln16_mt2_sr3; mg1_ln16_mt2_sr9; mg1_ln16_mt2_sr1; mg1_ln16_mt2_sr2; mg1_ln17_mt2_sr7; mg1_ln17_mt2_sr5; mg1_ln17_mt2_sr3; mg1_ln17_mt2_sr9; mg1_ln17_mt2_sr1; mg1_ln17_mt2_sr2; mg1_ln18_mt2_sr7; mg1_ln18_mt2_sr5; mg1_ln18_mt2_sr3; mg1_ln18_mt2_sr9; mg1_ln18_mt2_sr1; mg1_ln18_mt2_sr2; mg1_ln9_mt1_sr7; mg1_ln9_mt1_sr5; mg1_ln9_mt1_sr3; mg1_ln9_mt1_sr9; mg1_ln9_mt1_sr1; mg1_ln9_mt1_sr2; mg2_ln10_mt1_sr7; mg2_ln10_mt1_sr5; mg2_ln10_mt1_sr9; mg2_ln10_mt1_sr1; mg2_ln10_mt1_sr2; mg2_ln14_mt2_sr7; mg2_ln14_mt2_sr5; mg2_ln14_mt2_sr3; mg2_ln14_mt2_sr9; mg2_ln14_mt2_sr1; mg2_ln14_mt2_sr2; mg2_ln15_mt2_sr7; mg2_ln15_mt2_sr5; mg2_ln15_mt2_sr3; mg2_ln15_mt2_sr9; mg2_ln15_mt2_sr1; mg2_ln15_mt2_sr2; mg2_ln16_mt2_sr7; mg2_ln16_mt2_sr5; mg2_ln16_mt2_sr3; mg2_ln16_mt2_sr9; mg2_ln16_mt2_sr1; mg2_ln16_mt2_sr2; mg2_ln17_mt2_sr7; mg2_ln17_mt2_sr5; mg2_ln17_mt2_sr3; mg2_ln17_mt2_sr9; mg2_ln17_mt2_sr1; mg2_ln17_mt2_sr2; mg2_ln9_mt1_sr3; mg2_ln9_mt1_sr2; mg3_ln9_mt1_sr1; mg3_ln9_mt1_sr2; mg0_ln10_mt1_sr5; mg0_ln10_mt1_sr3; mg1_ln13_mt2_sr1; mg2_ln10_mt1_sr3; mg2_ln9_mt1_sr1; mg3_ln9_mt1_sr3; mg0_ln10_mt1_sr1; mg0_ln10_mt1_sr2; mg1_ln13_mt2_sr7; mg1_ln13_mt2_sr5; mg1_ln13_mt2_sr9; mg3_ln9_mt1_sr7; mg3_ln9_mt1_sr5; mg3_ln9_mt1_sr9; mg1_ln13_mt2_sr3; mg2_ln13_mt2_sr1; mg1_ln13_mt2_sr2; mg2_ln13_mt2_sr2; mg2_ln13_mt2_sr7; mg2_ln13_mt2_sr5; mg2_ln13_mt2_sr9; mg2_ln13_mt2_sr3; mg2_ln9_mt1_sr7; mg2_ln9_mt1_sr5; mg2_ln9_mt1_sr9
3	mg3_ln18_mt2_sr7; mg3_ln18_mt2_sr5; mg3_ln18_mt2_sr3; mg3_ln18_mt2_sr9; mg3_ln18_mt2_sr1; mg3_ln18_mt2_sr2; mg1_ln18_mt0_sr7; mg1_ln18_mt0_sr9; mg2_ln17_mt0_sr7; mg2_ln17_mt0_sr5; mg2_ln17_mt0_sr3; mg2_ln17_mt0_sr9; mg2_ln17_mt0_sr1; mg2_ln17_mt0_sr2; mg2_ln18_mt0_sr7; mg2_ln18_mt0_sr5; mg2_ln18_mt0_sr3; mg2_ln18_mt0_sr9; mg2_ln18_mt0_sr1; mg2_ln18_mt0_sr2; mg2_ln18_mt1_sr7; mg2_ln18_mt1_sr5; mg2_ln18_mt1_sr3; mg2_ln18_mt1_sr9; mg2_ln18_mt1_sr1; mg2_ln18_mt1_sr2; mg3_ln16_mt0_sr7; mg3_ln16_mt0_sr5; mg3_ln16_mt0_sr3; mg3_ln16_mt0_sr9; mg3_ln16_mt0_sr1; mg3_ln16_mt0_sr2; mg3_ln17_mt0_sr7; mg3_ln17_mt0_sr5; mg3_ln17_mt0_sr3; mg3_ln17_mt0_sr9; mg3_ln17_mt0_sr1; mg3_ln17_mt0_sr2; mg3_ln17_mt1_sr7; mg3_ln17_mt1_sr5; mg3_ln17_mt1_sr3; mg3_ln17_mt1_sr9; mg3_ln17_mt1_sr1; mg3_ln17_mt1_sr2; mg3_ln18_mt1_sr7; mg3_ln18_mt1_sr5; mg3_ln18_mt1_sr3; mg3_ln18_mt1_sr9; mg3_ln18_mt1_sr1; mg3_ln18_mt1_sr2; mg1_ln18_mt0_sr5; mg1_ln18_mt0_sr3; mg1_ln18_mt0_sr1; mg1_ln18_mt0_sr2; mg3_ln18_mt0_sr7; mg3_ln18_mt0_sr5; mg3_ln18_mt0_sr3; mg3_ln18_mt0_sr9; mg3_ln18_mt0_sr1; mg3_ln18_mt0_sr2
4	mg0_ln17_mt3_sr7; mg0_ln17_mt3_sr9; mg0_ln18_mt3_sr7; mg0_ln18_mt3_sr5; mg0_ln18_mt3_sr3; mg0_ln18_mt3_sr9; mg0_ln18_mt3_sr1; mg0_ln18_mt3_sr2; mg1_ln16_mt3_sr7; mg1_ln16_mt3_sr5; mg1_ln16_mt3_sr3; mg1_ln16_mt3_sr9; mg1_ln16_mt3_sr1; mg1_ln16_mt3_sr2; mg1_ln17_mt3_sr7; mg1_ln17_mt3_sr5; mg1_ln17_mt3_sr3; mg1_ln17_mt3_sr9; mg1_ln17_mt3_sr1; mg1_ln17_mt3_sr2; mg1_ln18_mt3_sr7; mg1_ln18_mt3_sr5; mg1_ln18_mt3_sr3; mg1_ln18_mt3_sr9; mg1_ln18_mt3_sr1; mg1_ln18_mt3_sr2; mg2_ln15_mt3_sr7; mg2_ln15_mt3_sr5; mg2_ln15_mt3_sr3; mg2_ln15_mt3_sr9; mg2_ln15_mt3_sr2; mg2_ln16_mt3_sr7; mg2_ln16_mt3_sr5; mg2_ln16_mt3_sr3; mg2_ln16_mt3_sr9; mg2_ln16_mt3_sr1; mg2_ln16_mt3_sr2; mg2_ln17_mt3_sr7; mg2_ln17_mt3_sr5; mg2_ln17_mt3_sr3; mg2_ln17_mt3_sr9; mg2_ln17_mt3_sr1; mg2_ln17_mt3_sr2; mg0_ln17_mt3_sr5; mg0_ln17_mt3_sr3; mg2_ln15_mt3_sr1; mg0_ln17_mt3_sr1; mg0_ln17_mt3_sr2; mg3_ln15_mt3_sr1; mg3_ln16_mt3_sr1
5	mg2_ln12_mt2_sr1; mg3_ln12_mt2_sr1; mg3_ln13_mt2_sr1; mg3_ln14_mt2_sr7; mg3_ln14_mt2_sr5; mg3_ln14_mt2_sr3; mg3_ln14_mt2_sr9; mg3_ln14_mt2_sr1; mg3_ln14_mt2_sr2; mg3_ln15_mt2_sr7; mg3_ln15_mt2_sr5; mg3_ln15_mt2_sr3; mg3_ln15_mt2_sr9; mg3_ln15_mt2_sr1; mg3_ln15_mt2_sr2; mg2_ln18_mt3_sr7; mg2_ln18_mt3_sr9; mg3_ln16_mt2_sr7; mg3_ln16_mt2_sr5; mg3_ln16_mt2_sr3; mg3_ln16_mt2_sr9; mg3_ln16_mt2_sr1; mg3_ln16_mt2_sr2; mg3_ln18_mt3_sr7; mg3_ln18_mt3_sr5; mg3_ln18_mt3_sr3; mg3_ln18_mt3_sr9; mg3_ln18_mt3_sr1; mg3_ln18_mt3_sr2; mg2_ln18_mt3_sr5; mg2_ln18_mt3_sr3; mg2_ln18_mt3_sr1; mg2_ln18_mt3_sr2; mg3_ln13_mt2_sr7; mg3_ln13_mt2_sr5; mg3_ln13_mt2_sr3; mg3_ln13_mt2_sr9; mg3_ln13_mt2_sr2
6	mg0_ln12_mt2_sr7; mg0_ln12_mt2_sr9; mg0_ln13_mt2_sr7; mg0_ln13_mt2_sr5; mg0_ln13_mt2_sr9; mg0_ln12_mt2_sr5; mg0_ln12_mt2_sr3; mg0_ln13_mt2_sr3; mg0_ln13_mt2_sr2; mg0_ln12_mt2_sr1; mg0_ln12_mt2_sr2; mg0_ln13_mt2_sr1; mg1_ln12_mt2_sr7; mg1_ln12_mt2_sr5; mg1_ln12_mt2_sr9; mg1_ln12_mt2_sr1; mg1_ln12_mt2_sr2; mg1_ln12_mt2_sr3

7	mg2_ln12_mt2_sr7; mg2_ln12_mt2_sr9; mg3_ln11_mt2_sr3; mg3_ln12_mt2_sr3; mg3_ln12_mt2_sr2; mg2_ln12_mt2_sr5; mg2_ln12_mt2_sr3; mg3_ln11_mt2_sr2; mg3_ln12_mt2_sr7; mg3_ln12_mt2_sr5; mg3_ln12_mt2_sr9; mg2_ln12_mt2_sr2; mg3_ln11_mt2_sr1
8	mg0_ln14_mt3_sr7; mg0_ln14_mt3_sr9; mg0_ln14_mt3_sr5; mg0_ln14_mt3_sr3; mg0_ln15_mt3_sr7; mg0_ln15_mt3_sr5; mg0_ln15_mt3_sr3; mg0_ln15_mt3_sr9; mg0_ln15_mt3_sr1; mg0_ln15_mt3_sr2; mg0_ln14_mt3_sr1; mg0_ln14_mt3_sr2
9	mg0_ln16_mt3_sr7; mg0_ln16_mt3_sr9; mg1_ln15_mt3_sr7; mg1_ln15_mt3_sr5; mg1_ln15_mt3_sr3; mg1_ln15_mt3_sr9; mg1_ln15_mt3_sr1; mg1_ln15_mt3_sr2; mg0_ln16_mt3_sr5; mg0_ln16_mt3_sr3; mg0_ln16_mt3_sr1; mg0_ln16_mt3_sr2
10	mg0_ln17_mt4_sr7; mg0_ln17_mt4_sr9; mg0_ln18_mt4_sr7; mg0_ln18_mt4_sr5; mg0_ln18_mt4_sr9; mg0_ln17_mt4_sr5; mg0_ln17_mt4_sr3; mg0_ln18_mt4_sr1; mg0_ln18_mt4_sr2; mg0_ln17_mt4_sr1; mg0_ln17_mt4_sr2; mg0_ln18_mt4_sr3
11	mg1_ln17_mt4_sr7; mg1_ln17_mt4_sr9; mg1_ln18_mt4_sr7; mg1_ln18_mt4_sr5; mg1_ln18_mt4_sr3; mg1_ln18_mt4_sr9; mg1_ln18_mt4_sr1; mg1_ln18_mt4_sr2; mg1_ln17_mt4_sr5; mg1_ln17_mt4_sr3; mg1_ln17_mt4_sr1; mg1_ln17_mt4_sr2
12	mg2_ln16_mt4_sr7; mg2_ln16_mt4_sr9; mg2_ln17_mt4_sr7; mg2_ln17_mt4_sr5; mg2_ln17_mt4_sr3; mg2_ln17_mt4_sr9; mg2_ln16_mt4_sr5; mg2_ln16_mt4_sr3; mg2_ln17_mt4_sr1; mg2_ln17_mt4_sr2; mg2_ln16_mt4_sr1; mg2_ln16_mt4_sr2
13	mg2_ln18_mt4_sr7; mg2_ln18_mt4_sr9; mg3_ln17_mt4_sr3; mg3_ln17_mt4_sr2; mg2_ln18_mt4_sr5; mg2_ln18_mt4_sr3; mg3_ln17_mt4_sr1; mg2_ln18_mt4_sr1; mg2_ln18_mt4_sr2; mg3_ln17_mt4_sr7; mg3_ln17_mt4_sr9; mg3_ln17_mt4_sr5
14	mg0_ln11_mt4_sr9; mg0_ln12_mt5_sr7; mg0_ln12_mt5_sr9; mg0_ln9_mt3_sr9; mg1_ln11_mt4_sr9; mg1_ln12_mt5_sr9; mg1_ln9_mt3_sr9; mg2_ln12_mt5_sr9; mg2_ln13_mt5_sr9; mg3_ln12_mt5_sr7; mg3_ln12_mt5_sr9
15	mg3_ln15_mt3_sr7; mg3_ln15_mt3_sr9; mg3_ln16_mt3_sr7; mg3_ln16_mt3_sr5; mg3_ln16_mt3_sr3; mg3_ln16_mt3_sr9; mg3_ln16_mt3_sr2; mg3_ln15_mt3_sr5; mg3_ln15_mt3_sr3; mg3_ln15_mt3_sr2
16	mg0_ln11_mt2_sr7; mg0_ln11_mt2_sr9; mg0_ln11_mt2_sr5; mg0_ln11_mt2_sr3; mg0_ln11_mt2_sr1; mg0_ln11_mt2_sr2
17	mg0_ln15_mt4_sr7; mg0_ln15_mt4_sr9; mg0_ln15_mt4_sr5; mg0_ln15_mt4_sr3; mg0_ln15_mt4_sr1; mg0_ln15_mt4_sr2
18	mg0_ln16_mt4_sr7; mg0_ln16_mt4_sr9; mg0_ln16_mt4_sr5; mg0_ln16_mt4_sr3; mg0_ln16_mt4_sr1; mg0_ln16_mt4_sr2
19	mg0_ln17_mt5_sr7; mg0_ln17_mt5_sr9; mg0_ln17_mt5_sr5; mg0_ln17_mt5_sr3; mg0_ln17_mt5_sr1; mg0_ln17_mt5_sr2
20	mg0_ln18_mt5_sr7; mg0_ln18_mt5_sr9; mg0_ln18_mt5_sr5; mg0_ln18_mt5_sr3; mg0_ln18_mt5_sr1; mg0_ln18_mt5_sr2
21	mg0_ln6_mt0_sr7; mg0_ln6_mt0_sr9; mg0_ln6_mt0_sr5; mg0_ln6_mt0_sr3; mg0_ln6_mt0_sr1; mg0_ln6_mt0_sr2
22	mg0_ln9_mt1_sr7; mg0_ln9_mt1_sr9; mg0_ln9_mt1_sr5; mg0_ln9_mt1_sr3; mg0_ln9_mt1_sr1; mg0_ln9_mt1_sr2
23	mg1_ln14_mt3_sr7; mg1_ln14_mt3_sr9; mg1_ln14_mt3_sr5; mg1_ln14_mt3_sr3; mg1_ln14_mt3_sr1; mg1_ln14_mt3_sr2
24	mg2_ln14_mt3_sr1; mg2_ln14_mt3_sr2; mg2_ln14_mt3_sr7; mg2_ln14_mt3_sr9; mg2_ln14_mt3_sr5; mg2_ln14_mt3_sr3
25	mg1_ln15_mt4_sr7; mg1_ln15_mt4_sr9; mg1_ln15_mt4_sr5; mg1_ln15_mt4_sr3; mg1_ln15_mt4_sr1; mg1_ln15_mt4_sr2
26	mg1_ln16_mt4_sr7; mg1_ln16_mt4_sr9; mg1_ln16_mt4_sr5; mg1_ln16_mt4_sr3; mg1_ln16_mt4_sr1; mg1_ln16_mt4_sr2

27	mg2_ln11_mt2_sr7; mg2_ln11_mt2_sr9; mg2_ln11_mt2_sr5; mg2_ln11_mt2_sr3; mg2_ln11_mt2_sr1; mg2_ln11_mt2_sr2
28	mg3_ln17_mt3_sr1; mg3_ln17_mt3_sr7; mg3_ln17_mt3_sr9; mg3_ln17_mt3_sr5; mg3_ln17_mt3_sr3; mg3_ln17_mt3_sr2
29	mg2_ln18_mt5_sr7; mg2_ln18_mt5_sr9; mg2_ln18_mt5_sr5; mg2_ln18_mt5_sr3; mg2_ln18_mt5_sr1; mg2_ln18_mt5_sr2
30	mg3_ln16_mt4_sr7; mg3_ln16_mt4_sr9; mg3_ln16_mt4_sr5; mg3_ln16_mt4_sr3; mg3_ln16_mt4_sr1; mg3_ln16_mt4_sr2
31	mg3_ln17_mt2_sr7; mg3_ln17_mt2_sr9; mg3_ln17_mt2_sr5; mg3_ln17_mt2_sr3; mg3_ln17_mt2_sr1; mg3_ln17_mt2_sr2
32	mg3_ln18_mt4_sr7; mg3_ln18_mt4_sr9; mg3_ln18_mt4_sr5; mg3_ln18_mt4_sr3; mg3_ln18_mt4_sr1; mg3_ln18_mt4_sr2
33	mg0_ln13_mt3_sr7; mg0_ln13_mt3_sr9; mg0_ln13_mt3_sr5; mg0_ln13_mt3_sr3; mg0_ln13_mt3_sr2
34	mg0_ln16_mt5_sr7; mg0_ln16_mt5_sr9; mg0_ln16_mt5_sr5; mg0_ln16_mt5_sr3; mg0_ln16_mt5_sr2
35	mg3_ln8_mt1_sr7; mg3_ln8_mt1_sr9; mg3_ln8_mt1_sr5; mg3_ln8_mt1_sr3; mg3_ln8_mt1_sr2
36	mg0_ln12_mt3_sr7; mg0_ln12_mt3_sr9; mg0_ln12_mt3_sr5; mg0_ln12_mt3_sr3
37	mg0_ln18_mt6_sr3; mg0_ln18_mt6_sr5; mg0_ln18_mt6_sr1; mg0_ln18_mt6_sr2
38	mg1_ln12_mt3_sr7; mg1_ln12_mt3_sr9; mg1_ln12_mt3_sr5; mg1_ln12_mt3_sr3
39	mg1_ln18_mt5_sr7; mg1_ln18_mt5_sr9; mg1_ln18_mt5_sr5; mg1_ln18_mt5_sr3
40	mg2_ln8_mt1_sr7; mg2_ln8_mt1_sr9; mg2_ln8_mt1_sr5; mg2_ln8_mt1_sr3
41	mg3_ln15_mt4_sr3; mg3_ln15_mt4_sr5; mg3_ln15_mt4_sr1; mg3_ln15_mt4_sr2
42	mg3_ln18_mt5_sr7; mg3_ln18_mt5_sr9; mg3_ln18_mt5_sr5; mg3_ln18_mt5_sr3
43	mg0_ln14_mt4_sr7; mg0_ln14_mt4_sr9; mg0_ln14_mt4_sr5
44	mg0_ln8_mt1_sr7; mg0_ln8_mt1_sr9; mg0_ln8_mt1_sr5
45	mg1_ln11_mt2_sr7; mg1_ln11_mt2_sr9; mg1_ln11_mt2_sr5
46	mg1_ln11_mt2_sr1; mg1_ln11_mt2_sr3; mg1_ln11_mt2_sr2
47	mg1_ln13_mt3_sr7; mg1_ln13_mt3_sr9; mg1_ln13_mt3_sr5
48	mg1_ln13_mt3_sr1; mg1_ln13_mt3_sr3; mg1_ln13_mt3_sr2
49	mg1_ln16_mt5_sr7; mg1_ln16_mt5_sr9; mg1_ln16_mt5_sr5

50	mg1_ln16_mt5_sr1; mg1_ln16_mt5_sr2; mg1_ln16_mt5_sr3
51	mg1_ln17_mt5_sr7; mg1_ln17_mt5_sr9; mg1_ln17_mt5_sr5
52	mg1_ln17_mt5_sr1; mg1_ln17_mt5_sr3; mg1_ln17_mt5_sr2
53	mg1_ln18_mt6_sr7; mg1_ln18_mt6_sr9; mg1_ln18_mt6_sr5
54	mg1_ln18_mt6_sr1; mg1_ln18_mt6_sr2; mg1_ln18_mt6_sr3
55	mg1_ln8_mt1_sr7; mg1_ln8_mt1_sr9; mg1_ln8_mt1_sr5
56	mg2_ln10_mt2_sr1; mg2_ln10_mt2_sr2; mg2_ln10_mt2_sr3
57	mg2_ln12_mt3_sr1; mg2_ln12_mt3_sr3; mg2_ln12_mt3_sr2
58	mg2_ln13_mt3_sr7; mg2_ln13_mt3_sr9; mg2_ln13_mt3_sr5
59	mg2_ln13_mt3_sr1; mg2_ln13_mt3_sr3; mg2_ln13_mt3_sr2
60	mg2_ln14_mt4_sr1; mg2_ln14_mt4_sr3; mg2_ln14_mt4_sr2
61	mg2_ln15_mt4_sr7; mg2_ln15_mt4_sr9; mg2_ln15_mt4_sr5
62	mg2_ln15_mt4_sr1; mg2_ln15_mt4_sr3; mg2_ln15_mt4_sr2
63	mg2_ln17_mt5_sr7; mg2_ln17_mt5_sr9; mg2_ln17_mt5_sr5
64	mg2_ln17_mt5_sr1; mg2_ln17_mt5_sr3; mg2_ln17_mt5_sr2
65	mg2_ln18_mt6_sr7; mg2_ln18_mt6_sr9; mg2_ln18_mt6_sr5
66	mg3_ln11_mt2_sr7; mg3_ln11_mt2_sr9; mg3_ln11_mt2_sr5
67	mg3_ln12_mt3_sr7; mg3_ln12_mt3_sr9; mg3_ln12_mt3_sr5
68	mg3_ln13_mt3_sr7; mg3_ln13_mt3_sr9; mg3_ln13_mt3_sr5
69	mg3_ln13_mt3_sr1; mg3_ln13_mt3_sr3; mg3_ln13_mt3_sr2
70	mg3_ln14_mt3_sr7; mg3_ln14_mt3_sr9; mg3_ln14_mt3_sr5
71	mg3_ln14_mt3_sr1; mg3_ln14_mt3_sr3; mg3_ln14_mt3_sr2
72	mg3_ln17_mt5_sr7; mg3_ln17_mt5_sr9; mg3_ln17_mt5_sr5

73	mg3_ln6_mt0_sr7; mg3_ln6_mt0_sr9; mg3_ln6_mt0_sr5
74	mg0_ln10_mt2_sr7; mg0_ln10_mt2_sr9
75	mg0_ln13_mt4_sr7; mg0_ln13_mt4_sr9
76	mg0_ln13_mt5_sr7; mg0_ln13_mt5_sr9
77	mg0_ln14_mt4_sr3; mg0_ln14_mt4_sr2
78	mg0_ln18_mt6_sr7; mg0_ln18_mt6_sr9
79	mg0_ln8_mt1_sr2; mg0_ln8_mt1_sr3
80	mg1_ln10_mt2_sr7; mg1_ln10_mt2_sr9
81	mg1_ln14_mt4_sr7; mg1_ln14_mt4_sr9
82	mg1_ln14_mt4_sr2; mg1_ln14_mt4_sr3
83	mg1_ln15_mt5_sr3; mg1_ln15_mt5_sr5
84	mg1_ln17_mt6_sr5; mg1_ln17_mt6_sr7
85	mg1_ln18_mt5_sr1; mg1_ln18_mt5_sr2
86	mg1_ln8_mt1_sr2; mg1_ln8_mt1_sr3
87	mg2_ln10_mt2_sr7; mg2_ln10_mt2_sr9
88	mg2_ln12_mt3_sr7; mg2_ln12_mt3_sr9
89	mg2_ln13_mt4_sr2; mg2_ln13_mt4_sr3
90	mg2_ln14_mt4_sr5; mg2_ln14_mt4_sr7
91	mg2_ln15_mt5_sr2; mg2_ln15_mt5_sr3
92	mg2_ln16_mt5_sr7; mg2_ln16_mt5_sr9
93	mg2_ln16_mt5_sr1; mg2_ln16_mt5_sr2
94	mg2_ln16_mt6_sr7; mg2_ln16_mt6_sr9
95	mg2_ln17_mt6_sr7; mg2_ln17_mt6_sr9

96	mg2_ln17_mt6_sr2; mg2_ln17_mt6_sr3
97	mg2_ln18_mt6_sr2; mg2_ln18_mt6_sr3
98	mg2_ln8_mt1_sr1; mg2_ln8_mt1_sr2
99	mg3_ln10_mt2_sr7; mg3_ln10_mt2_sr9
100	mg3_ln12_mt3_sr2; mg3_ln12_mt3_sr3
101	mg3_ln14_mt4_sr7; mg3_ln14_mt4_sr9
102	mg3_ln14_mt4_sr2; mg3_ln14_mt4_sr3
103	mg3_ln15_mt4_sr7; mg3_ln15_mt4_sr9
104	mg3_ln16_mt5_sr7; mg3_ln16_mt5_sr9
105	mg3_ln16_mt5_sr2; mg3_ln16_mt5_sr3
106	mg3_ln17_mt5_sr1; mg3_ln17_mt5_sr2
107	mg3_ln18_mt5_sr1; mg3_ln18_mt5_sr2
108	mg3_ln18_mt6_sr5; mg3_ln18_mt6_sr7

Legend: Primer set - APC composition of each cluster classified based on the index of 99% or more match of template amplification prediction.

Supplementary Table 6: APC properties of each cluster

cluster number	number of APC	mg	ln	mt	sr
1	435	0; 1; 2; 3	6; 7; 8; 9; 10; 11; 12; 13; 14; 15; 16; 17; 18	0; 1; 2	1; 2; 3; 5; 7; 9
2	150	0; 1; 2; 3	9; 10; 11; 12; 13; 14; 15; 16; 17; 18	1; 2	1; 2; 3; 5; 7; 9
3	60	1; 2; 3	16; 17; 18	0; 1; 2	1; 2; 3; 5; 7; 9
4	50	0; 1; 2; 3	15; 16; 17; 18	3	1; 2; 3; 5; 7; 9
5	38	2; 3	12; 13; 14; 15; 16; 18	2; 3	1; 2; 3; 5; 7; 9
6	18	0; 1	12; 13	2	1; 2; 3; 5; 7; 9
7	13	2; 3	11; 12	2	1; 2; 3; 5; 7; 9
8	12	0	14; 15	3	1; 2; 3; 5; 7; 9
9	12	0; 1	15; 16	3	1; 2; 3; 5; 7; 9
10	12	0	17; 18	4	1; 2; 3; 5; 7; 9
11	12	1	17; 18	4	1; 2; 3; 5; 7; 9
12	12	2	16; 17	4	1; 2; 3; 5; 7; 9
13	12	2; 3	17; 18	4	1; 2; 3; 5; 7; 9
14	11	0; 1; 2; 3	9; 11; 12; 13	3; 4; 5	7; 9
15	10	3	15; 16	3	2; 3; 5; 7; 9
16	6	0	11	2	1; 2; 3; 5; 7; 9
17	6	0	15	4	1; 2; 3; 5; 7; 9
18	6	0	16	4	1; 2; 3; 5; 7; 9
19	6	0	17	5	1; 2; 3; 5; 7; 9
20	6	0	18	5	1; 2; 3; 5; 7; 9
21	6	0	6	0	1; 2; 3; 5; 7; 9
22	6	0	9	1	1; 2; 3; 5; 7; 9

23	6	1	14	3	1; 2; 3; 5; 7; 9
24	6	2	14	3	1; 2; 3; 5; 7; 9
25	6	1	15	4	1; 2; 3; 5; 7; 9
26	6	1	16	4	1; 2; 3; 5; 7; 9
27	6	2	11	2	1; 2; 3; 5; 7; 9
28	6	3	17	3	1; 2; 3; 5; 7; 9
29	6	2	18	5	1; 2; 3; 5; 7; 9
30	6	3	16	4	1; 2; 3; 5; 7; 9
31	6	3	17	2	1; 2; 3; 5; 7; 9
32	6	3	18	4	1; 2; 3; 5; 7; 9
33	5	0	13	3	2; 3; 5; 7; 9
34	5	0	16	5	2; 3; 5; 7; 9
35	5	3	8	1	2; 3; 5; 7; 9
36	4	0	12	3	3; 5; 7; 9
37	4	0	18	6	1; 2; 3; 5
38	4	1	12	3	3; 5; 7; 9
39	4	1	18	5	3; 5; 7; 9
40	4	2	8	1	3; 5; 7; 9
41	4	3	15	4	1; 2; 3; 5
42	4	3	18	5	3; 5; 7; 9
43	3	0	14	4	5; 7; 9
44	3	0	8	1	5; 7; 9
45	3	1	11	2	5; 7; 9
46	3	1	11	2	1; 2; 3

47	3	1	13	3	5; 7; 9
48	3	1	13	3	1; 2; 3
49	3	1	16	5	5; 7; 9
50	3	1	16	5	1; 2; 3
51	3	1	17	5	5; 7; 9
52	3	1	17	5	1; 2; 3
53	3	1	18	6	5; 7; 9
54	3	1	18	6	1; 2; 3
55	3	1	8	1	5; 7; 9
56	3	2	10	2	1; 2; 3
57	3	2	12	3	1; 2; 3
58	3	2	13	3	5; 7; 9
59	3	2	13	3	1; 2; 3
60	3	2	14	4	1; 2; 3
61	3	2	15	4	5; 7; 9
62	3	2	15	4	1; 2; 3
63	3	2	17	5	5; 7; 9
64	3	2	17	5	1; 2; 3
65	3	2	18	6	5; 7; 9
66	3	3	11	2	5; 7; 9
67	3	3	12	3	5; 7; 9
68	3	3	13	3	5; 7; 9
69	3	3	13	3	1; 2; 3
70	3	3	14	3	5; 7; 9

71	3	3	14	3	1; 2; 3
72	3	3	17	5	5; 7; 9
73	3	3	6	0	5; 7; 9
74	2	0	10	2	7; 9
75	2	0	13	4	7; 9
76	2	0	13	5	7; 9
77	2	0	14	4	2; 3
78	2	0	18	6	7; 9
79	2	0	8	1	2; 3
80	2	1	10	2	7; 9
81	2	1	14	4	7; 9
82	2	1	14	4	2; 3
83	2	1	15	5	3; 5
84	2	1	17	6	5; 7
85	2	1	18	5	1; 2
86	2	1	8	1	2; 3
87	2	2	10	2	7; 9
88	2	2	12	3	7; 9
89	2	2	13	4	2; 3
90	2	2	14	4	5; 7
91	2	2	15	5	2; 3
92	2	2	16	5	7; 9
93	2	2	16	5	1; 2
94	2	2	16	6	7; 9

95	2	2	17	6	7; 9
96	2	2	17	6	2; 3
97	2	2	18	6	2; 3
98	2	2	8	1	1; 2
99	2	3	10	2	7; 9
100	2	3	12	3	2; 3
101	2	3	14	4	7; 9
102	2	3	14	4	2; 3
103	2	3	15	4	7; 9
104	2	3	16	5	7; 9
105	2	3	16	5	2; 3
106	2	3	17	5	1; 2
107	2	3	18	5	1; 2
108	2	3	18	6	5; 7

Legend: Primer set - number of constituent APCs and mg, ln, mt, and sr ranges of each cluster classified based on the index of 99% or higher match of template amplification prediction.

Supplementary Table 7: Representational image of the data table for PyCaret analysis

Primer set	Template	Experimental result	APC		
			mg0_ln10_mt0_sr7	mg0_ln10_mt1_sr7	mg3_ln18_mt2_sr7
12	1	1	0	0	1
12	2	0	0	1	0
12	3	1	0	0	0
12	4	1	0	0	1
12	5	1	0	1	0
13	1	1	1	1	0
13	2	1	0	1	0
13	3	0	1	1	1
13	4	1	0	0	1
13	5	1	0	1	1

Legend: An example (partial) of a data table for input into PyCaret. Blue indicates row settings (primer set - template), red indicates target setting columns, and yellow indicates training data.

Supplementary Figure 1: Classification of Amplification Patterns in LAMP Experiments

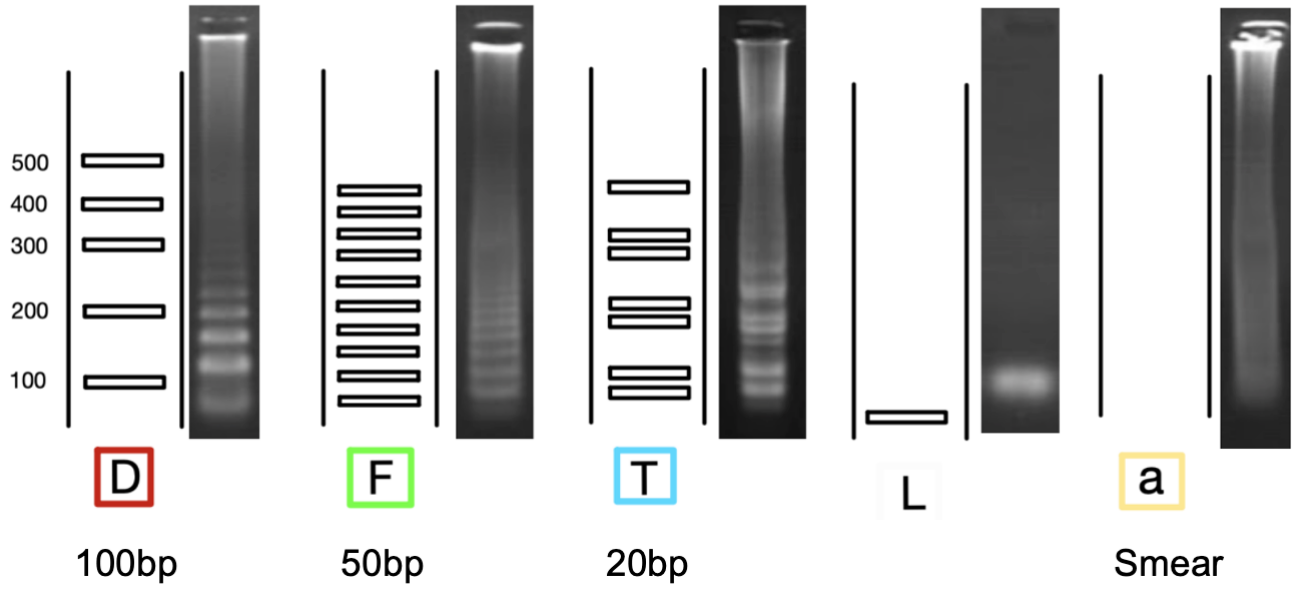

Legend: LAMP amplification patterns can be divided into the following five categories (1) a ladder with every 100 bp [named dumbbell ladder (D)] (2) a ladder with every 20 bp between bands [named double dumbbell ladder (T)] (3) a ladder with every 50 bp [named (F)] (4) a single band with every 50 bp [named (L)] (5) a smeared one [named (a)].

Supplementary Figure 2: Schematic diagram of LAMP amplification

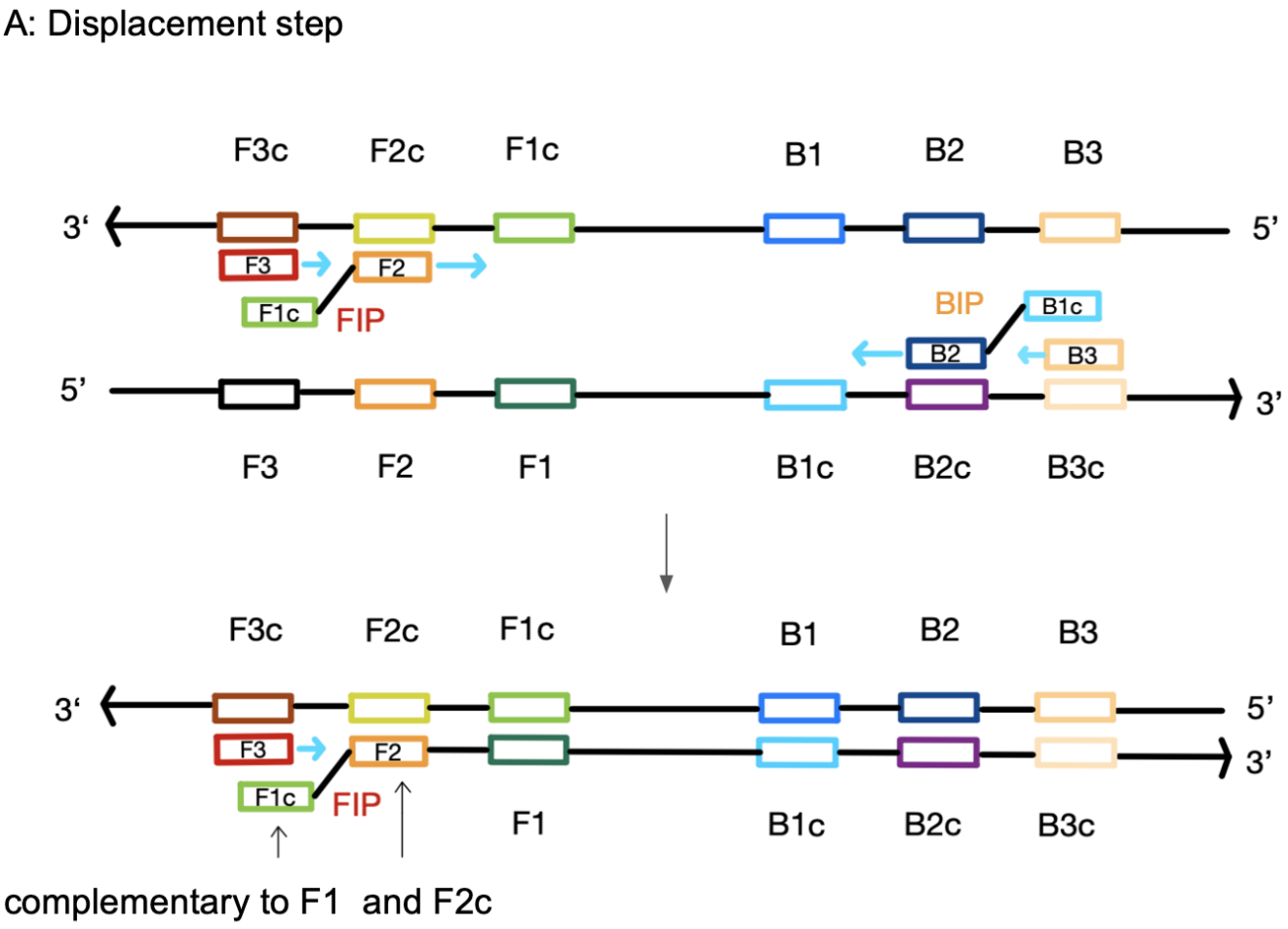

B: Formation of single-strand DNA and dumbbell-like structure

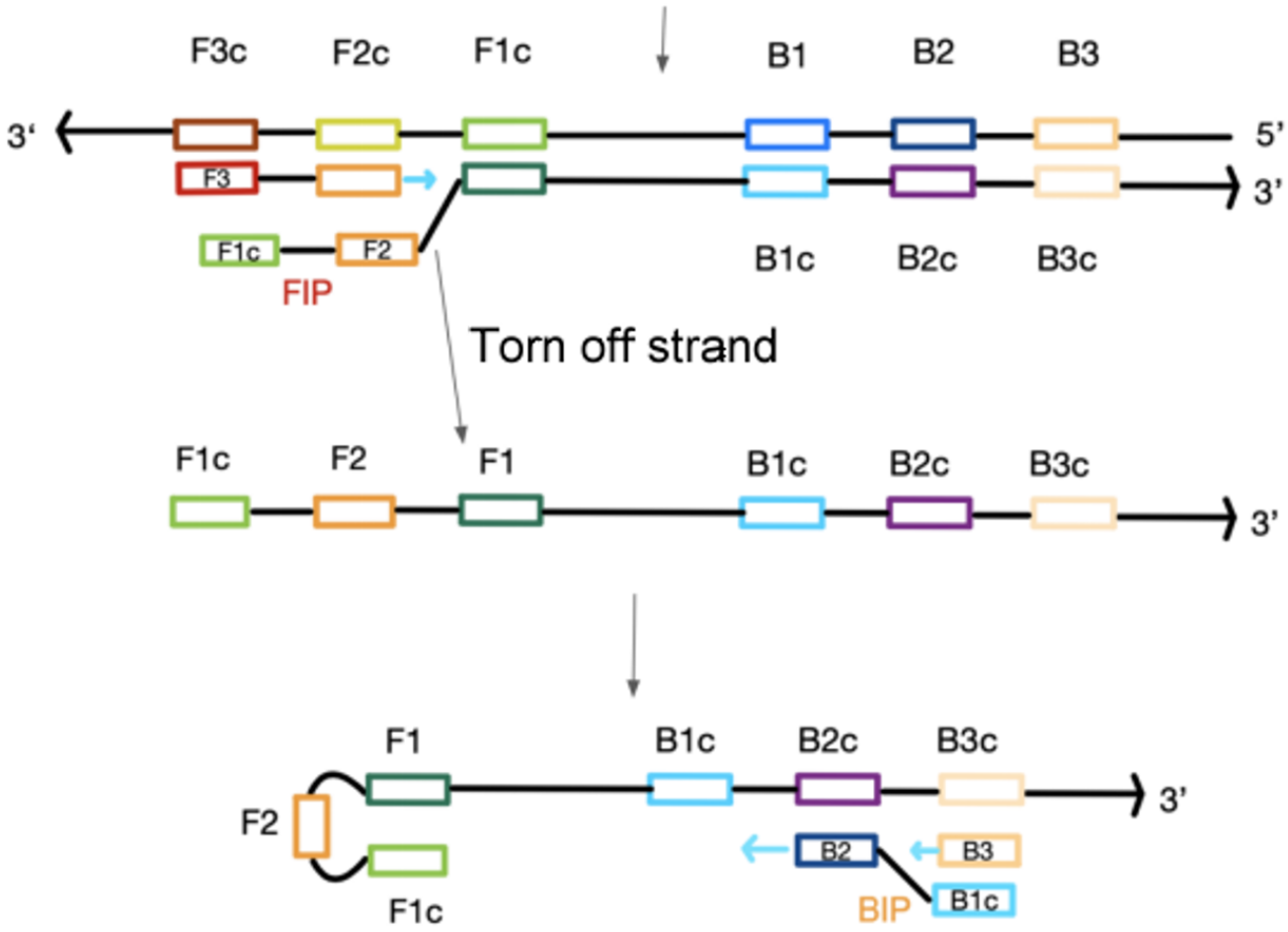

C: Disappearance of B3-primer binding site through loop formation

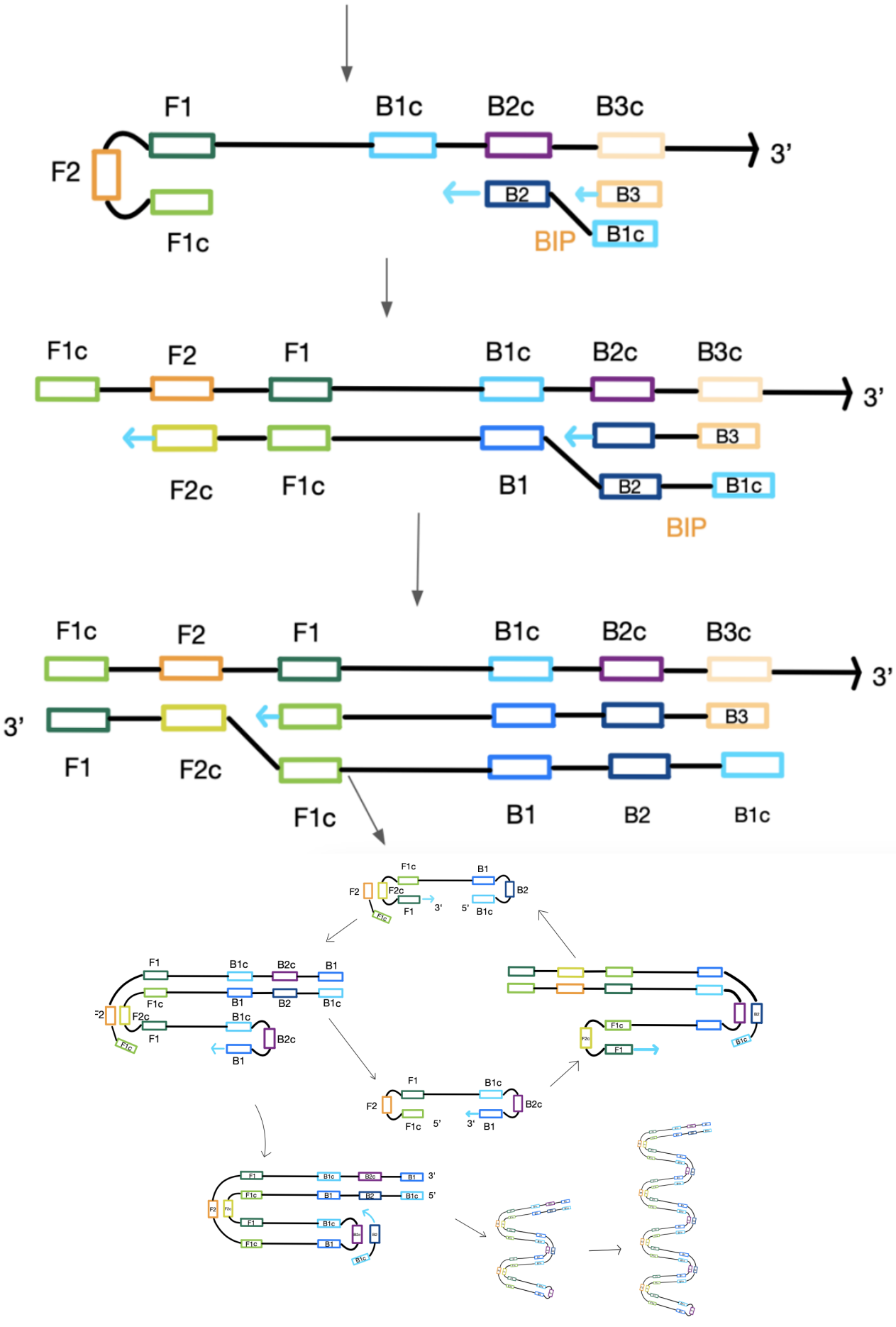

Supplementary Figure 3: Schematic positions of regions in primers

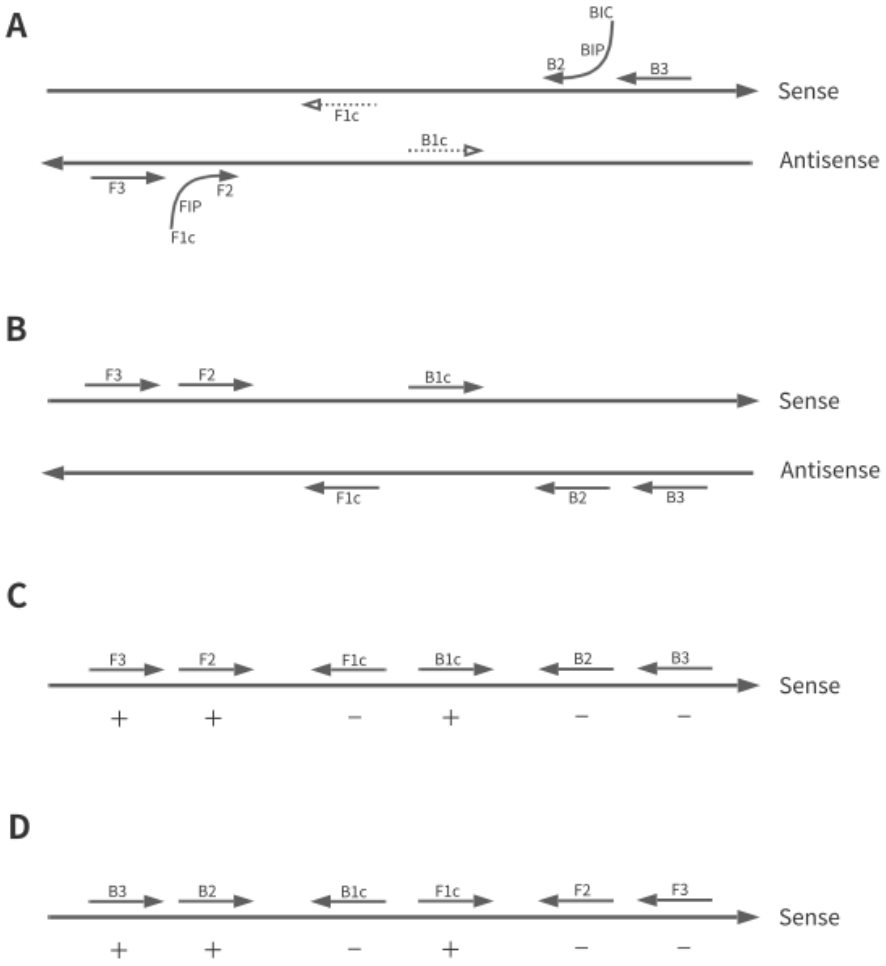

Supplementary Figure 4: Schematic presentation of the conditions for feature formation regions

A. Cutout conditions for the calculation of feature-data

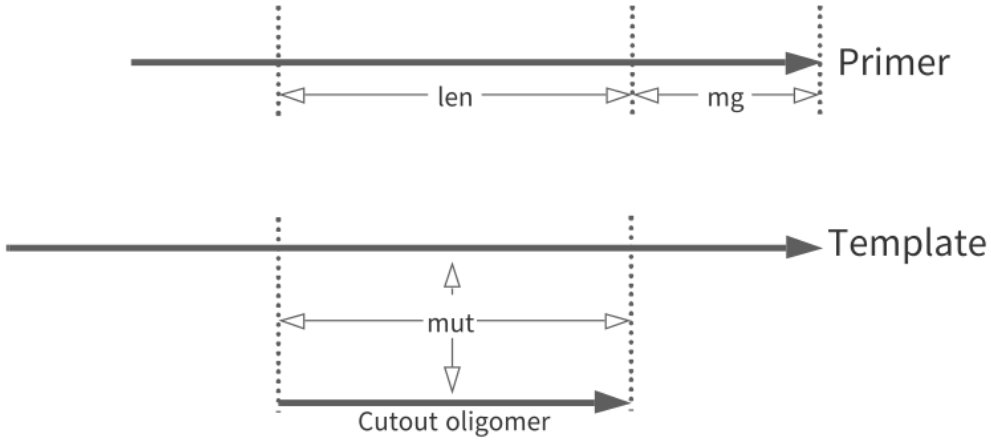

B. Examples for the mlms homology search

Primer: lamp_16s_21_F3, Sequence: CACAGGTGGTGCATGGTC

For homology search “mg2_ln7_mt1_sr2”

Target sequence (bold black 7mer cut with 2-base margin): CACAGGTGG**TGCATGG**TC

+ Sense homology on sense strand of template 5:

Start and End positions of homology		Template sequence	mt	Homologous character (Supplementary Table 4)
106	112	GCCCGCA	1	E
350	356	TTCCGCA	1	E

Alignment of homologies of cutout 7 mers from F1c, F2, F3, B1c, B2, B3 on the template 5 (example data).

Notations are according to Supplementary Table 4.

Homologies on the sense template: F3+, F1c+, F2+, F1c-, B1c+, F2+, B3-, B2-, B3-

Homology characters (Red: Amplifiable alignment of characters): EACBGCLJL

sr2 means amplifiability permit A in EAC and CL in GCLJ

Supplementary Figure 5: Clustering method for APC

A. Coincidence of amplification-prediction for each primer-template and APC

Prediction of amplification for each primer-template							APC
Template **Primer**	**1**	**2**	**3**	**4**	**5**		
12	×	×	×	×	×		mg0_ln10_mt0_sr7
13	○	×	○	×	×		mg1_ln13_mt0_sr9
14	○	○	○	○	○		mg1_ln8_mt0_sr9
15	○	×	×	○	○		.
16	○	×	×	○	○		.
Template **Primer**	**1**	**2**	**3**	**4**	**5**		
12	×	○	×	×	○		mg0_ln10_mt1_sr7
13	○	○	○	×	○		mg1_ln14_mt2_sr5
14	○	○	○	○	×		mg2_ln10_mt1_sr3
15	○	×	×	×	×		.
16	×	×	×	×	×		.

Template Primer	1	2	3	4	5		
12	○	×	×	○	×		mg3_ln18_mt2_sr7
13	×	×	○	○	○		mg2_ln17_mt0_sr9
14	×	○	○	○	×		mg3_ln16_mt0_sr3
15	○	×	×	×	×		.
16	×	×	×	×	×		.

B. MCL-clustering method

1) ABC-format relation of APCs

mg0_ln10_mt0_sr7 mg1_ln13_mt0_sr9 1

mg1_ln13_mt0_sr9 mg1_ln8_mt0_sr9 1

mg0_ln10_mt1_sr7 mg1_ln14_mt2_sr5 1

mg1_ln14_mt2_sr5 mg2_ln10_mt1_sr3 1

mg3_ln18_mt2_sr7 mg2_ln17_mt0_sr9 1

mg2_ln17_mt0_sr9 mg3_ln16_mt0_sr3 1

2) MCL clustering result

Cluster number	APCs		
1	mg0_ln10_mt0_sr7	mg1_ln13_mt0_sr9	mg1_ln8_mt0_sr9
2	mg0_ln10_mt1_sr7	mg1_ln14_mt2_sr5	mg2_ln10_mt1_sr3
3	mg3_ln18_mt2_sr7	mg2_ln17_mt0_sr9	mg3_ln16_mt0_sr3

Legend: Primer set - APC cluster formation process based on amplification prediction for each template. A: The process of listing APCs with matching results based on amplification predictions. B: The process of calculating clusters using MCL assuming that some APCs with matching results overlap. 1) Enter the matching APC in ABC format on one line, and write the number 1 to indicate a match in the third column. 2) We show that the result is obtained as text data in which all APCs clustered by the MCL program are written on one line.